Chapter 15: Practical Strain Analysis

THE STUDY of deformed rocks may benefit from measurements to quantify the strain recorded in them. Knowledge of their state of strain may be useful, because it constrains the extension and shortening directions. This may help to explain the occurrence of various types of tectonites and deformation patterns of single competent and single incompetent layers. The amount of volume change, if any, can sometimes be assessed if the strain of the deformed rock can be compared with that of undeformed rocks nearby. The principal stretches (i.e., S_1, S_2, and S_3) determine the shape of the strain ellipsoid and the magnitude of the strain. This Chapter outlines methods to obtain the principal stretches from strain measurements from arbitrary outcrop surfaces.

Contents: The major types of marker objects, used for strain determinations, are outlined in section 15-1. The distinction of prolate, oblate, and plane strains on the basis of tectonite fabrics is outlined in sections 15-2 and 15-3. Section 15-4 formulates criteria for analyzing plane strain. Section 15-5 provides similar expressions for general 3D deformations. Section 15-6 considers volume changes, possibly involved in any 3D deformation. Sections 15-7 to 15-10 explain a selection of the most practical techniques available for strain analysis: (R_f/ϕ)-method, stretched line-method, Wellman method, Breddin method, Fry method, and tieline method. Finally, sections 15-11 to 15-13 outline how finite strain estimates are affected if the plane of study is oblique to the principal stretches.

Practical hint:
The theory of strain analysis, practiced in this chapter, is designed for application on natural outcrops of deformed rocks. An outdoor session of strain analysis on outcrops can be considered if suitable localities are available nearby.

15-1 Strain analysis

The strain ellipse is a graphical concept to visualize the amount of strain involved in the deformation of rocks. The strain concept is useful only at length scales for which the deformation can be considered uniform or homogeneous. For example, Figures 15-1a & b illustrate the formation of a folded layer from initially planar strata. The intensity of the deformation is spatially varying and inhomogeneous, but it is uniform if studied at the scale outlined by the deformed parallelopiped and the undeformed cube. A classical example of deformation analysis on small domains is provided by the measurements of Ernst Cloos on deformed ooids of folded

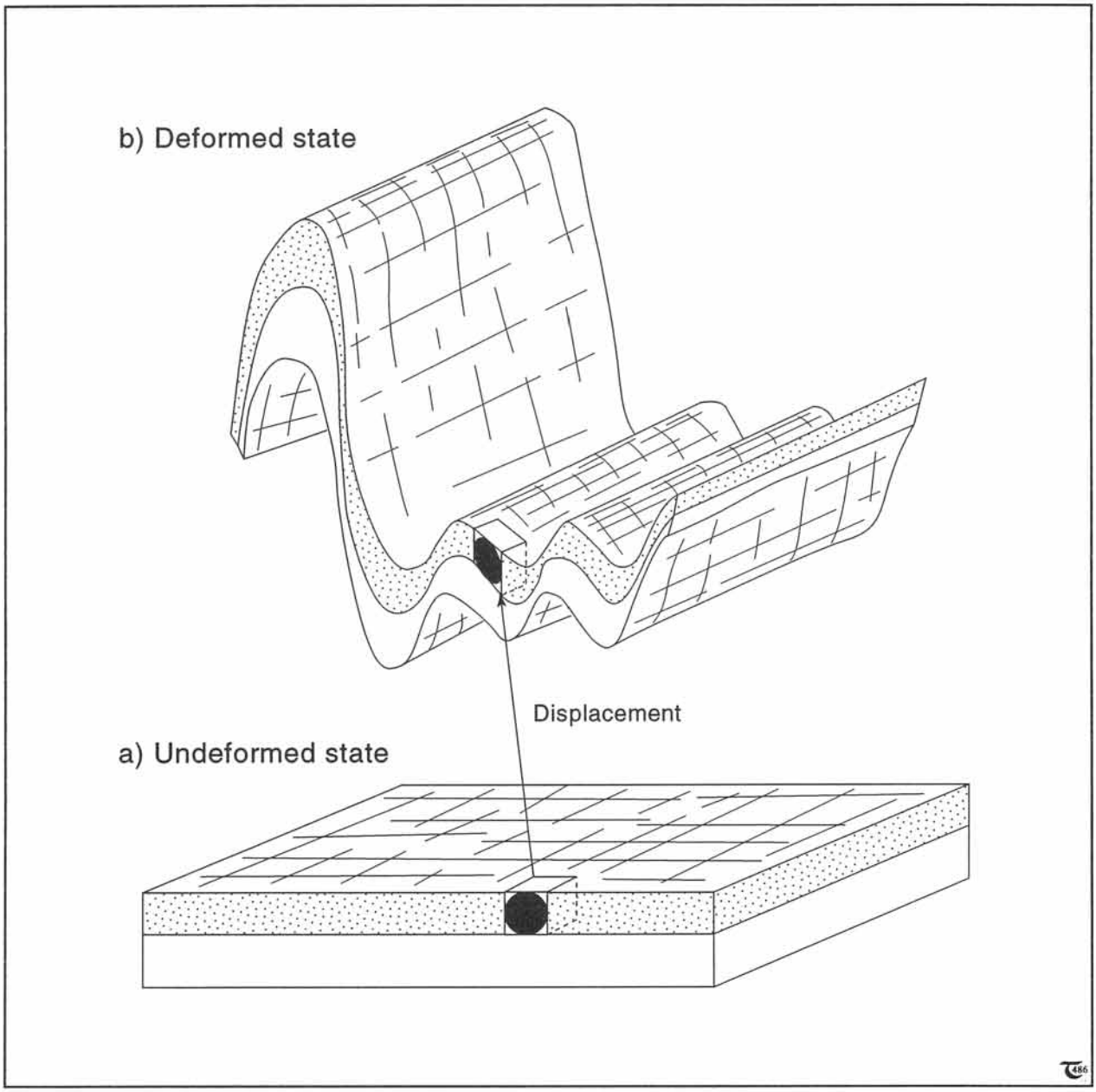

Figure 15-1: *a) & b) Undeformed and folded state of rock strata. The strain and rotation components of deformation changed the original unit cube into a parallelopiped.*

oolites in the South Mountain anticline, Maryland, USA (Figs. 15-2a & b).

The techniques and principles of strain analysis of rock deformation patterns have developed from the need to quantify the amount of distortion recorded within deformed rocks. The measurement of strain in the field is an extremely difficult, tedious, and time-consuming affair and is possible only under special conditions. This may explain why the number of practical strain studies performed in the field is still limited.

If all rocks would contain ooids of spherical initial shape, strain analysis would be relatively simple. In the absence of such spherical objects, a variety of other objects may be utilized as strain markers. Objects suitable for strain measurements can be grouped as follows: a) Initially spherical or circular objects: cylindrical worm tubes in orthogonal sections, reduction spots, ooids, pisolitic tuffs, spherulites, amygdules, vesicles, and concretion balls; b) Initially ellipsoidal or elliptical objects: conglomerate pebbles, volcanic bombs, lava pillows, and xenoliths; c) Initially linear objects: belemnites, crinoids, graptolites, large prismatic crystals, boudins, and ptygmatic folds; d) Objects with known angular features: fossils of bilateral symmetry such as trilobites and brachiopods; e) Evenly distributed objects: centers of mineral grains, pebbles, and other regularly spaced objects.

The result of any strain analysis is affected not only by the orientation of the plane of study (sections 15-11 to 15-13). Another effect, influencing the strain measurement, results from the difference in mechanical properties of the strain marker material and the host rock. Strain marker objects, such as the pebbles in a conglomerate, may locally affect the strain accumulation so much that the strains inferred deviate from the strain experienced by the rest of the rock volume. This possible complication must be carefully assessed in any particular strain analysis. In this context, the term *strain memory* is sometimes used to qualify how completely or incompletely

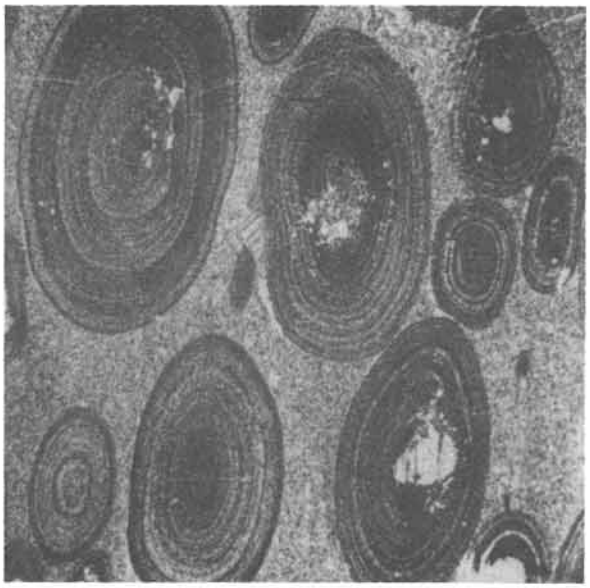

Figure 15-2a: *Example of thin section photograph of deformed ooids from South Mountain anticline, USA, studied by Ernst Cloos. Image is 2mm wide.*

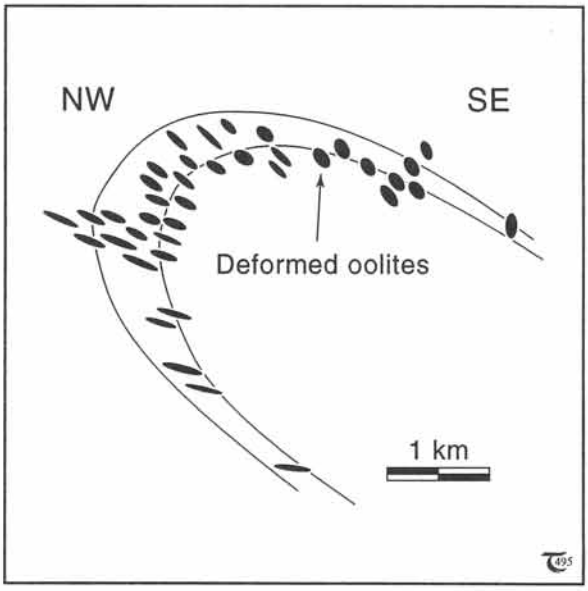

Figure 15-2b: *Strain pattern in the South Mountain anticline, Maryland, based on strain estimates from deformed ooids in thin section studies.*

the strain recorded in the rock represents the total strain undergone by that rock.

Finally, the most reliable strain analyses can be made in the laboratory on samples, carefully marked for their original orientation in the field. Cutting planes of the sample can be selected to coincide with the principal planes of strain, which can then be studied either in thin sections or on polished planes. It is most practical to work on enlarged photographs of either the thin sections or the polished surfaces.

☐Exercise 15-1: Explain what is meant if rocks have: a) complete or good strain memory, and b) incomplete or poor strain memory. c) Describe possible examples of rocks and their internal strain markers, which would qualify as either good or poor strain gauges.

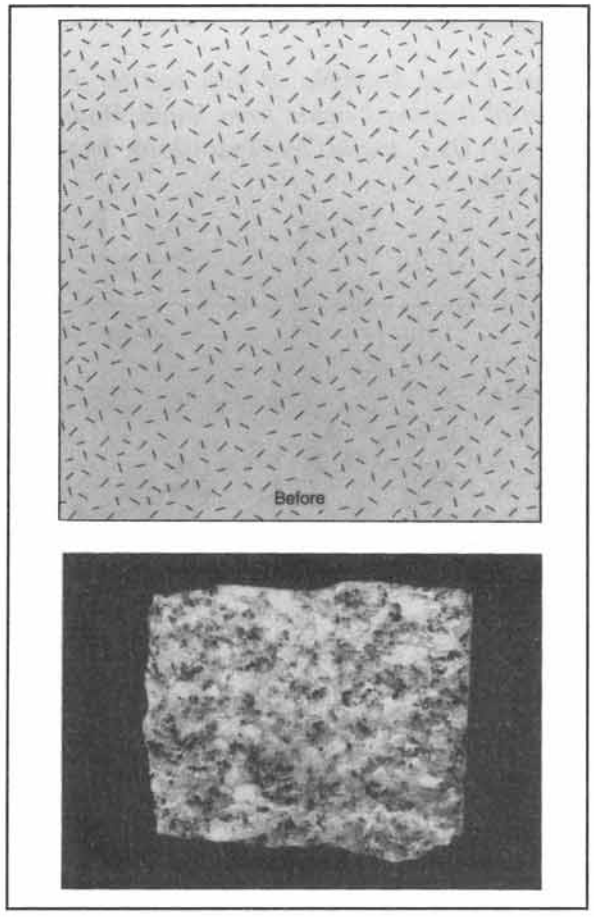

Figure 15-3a: *Sketch and photograph of isotropic fabric in undeformed granite. Sample is 10 cm across.*

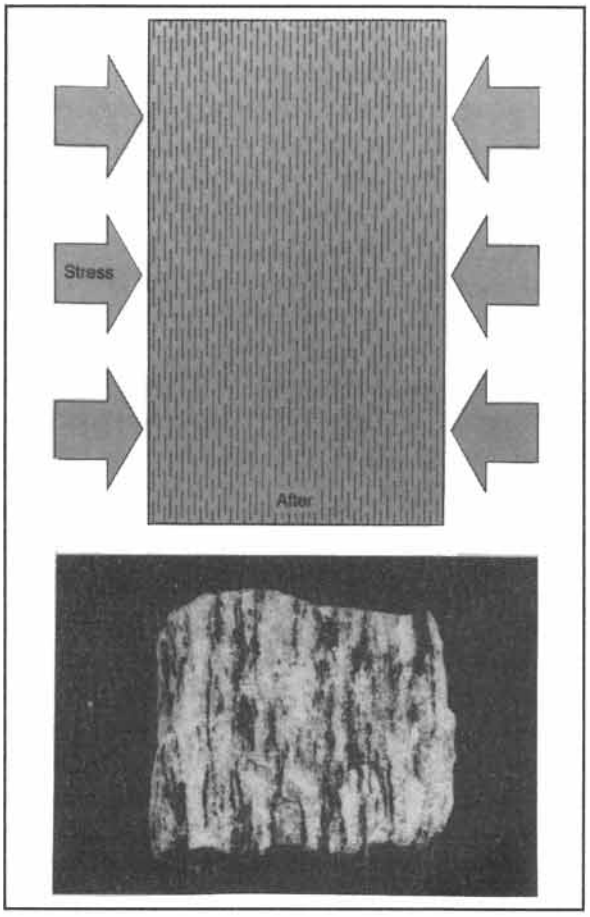

Figure 15-3b: *Anisotropic fabric, comprising compositional layering and grain shape orientation in gneiss, possibly due to shortening normal to the foliation plane. Sample is 10 cm across.*

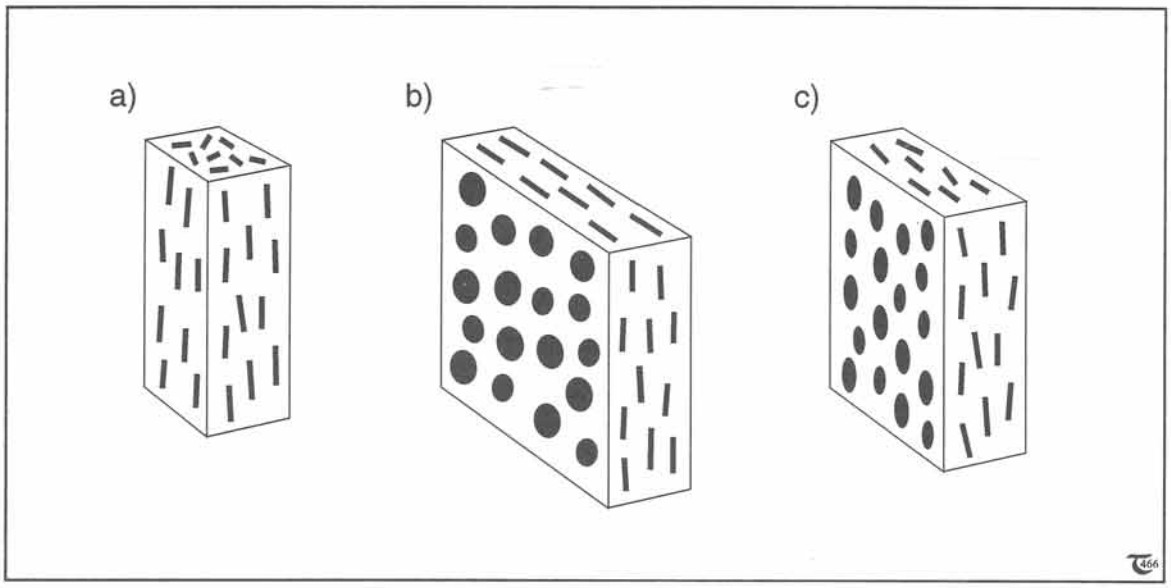

Figure 15-4: *a) to c) Three basic types of tectonites: (a) L-tectonite (prolate strain), (b) S-tectonite (oblate strain), and (c) L-S tectonite (plane strain).*

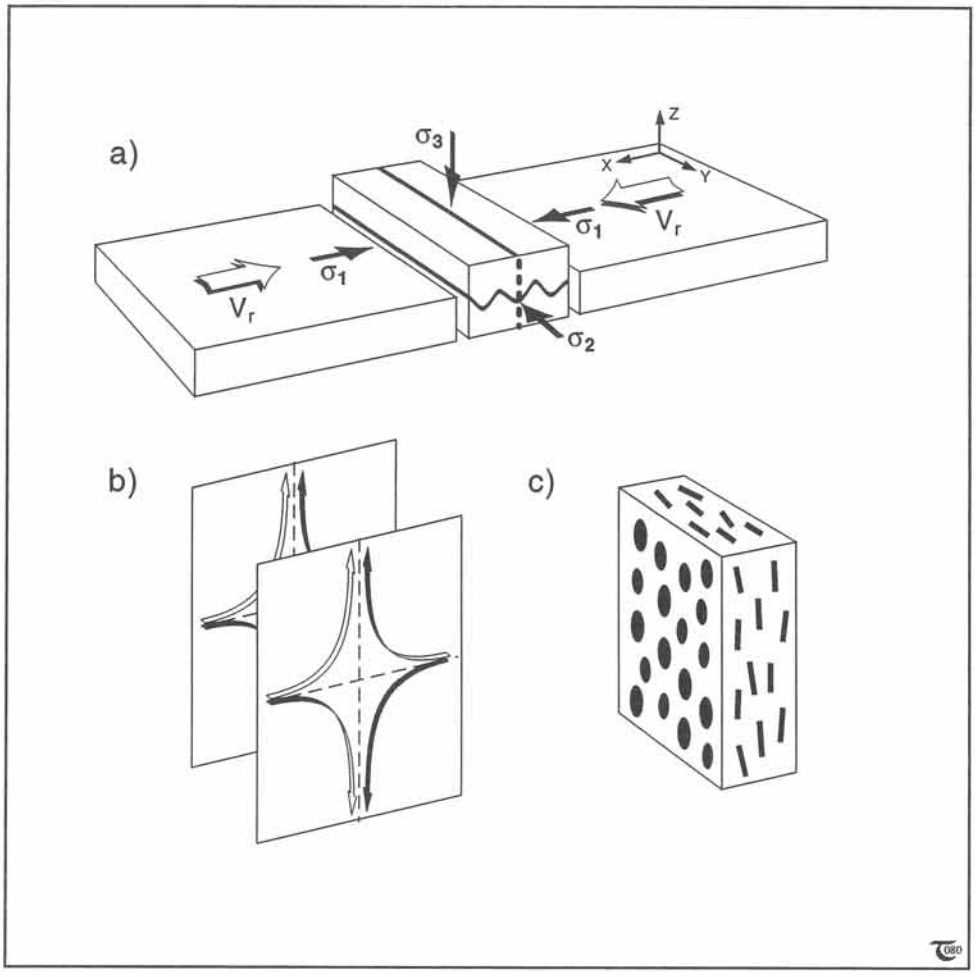

Figure 15-5: *a) Compressional pure shear between two colliding plates causing L-S tectonites. b) Streamline pattern inside the deformation zone. c) Both L and S are subvertical and normal to the shortening direction.*

15-2 Tectonites

A high intensity deformation is likely to transform any isotropic rock into an anisotropic rock by the development of a grain-shape fabric, which may include the formation of rock cleavage and lineation, due to the preferred alignment of platy and prismatic minerals (Figs. 15-3a & b). Bruno Sander suggested in the 1950's that the grain-shape fabric of deformed rocks will tend to align with the finite strain ellipsoid that represents the deformation of the bulk volume. He introduced the terms L-tectonite, S-tectonite, and L-S-tectonite. L-tectonites are deformed rocks, that possess a clear grain-shape fabric or preferred mineral orientation, which defines a lineation only, and in which any foliation is absent (Fig. 15-4a). S-tectonites are deformed rocks, possessing a penetrative foliation or schistosity, defined by the grain-shape fabric (Fig. 15-4b). L-S-tectonites display both a foliation and lineation (Fig. 15-4c). The application of Sander's assumption would imply that prolate deformations or constriction will produce L-tectonites, oblate deformation or flattening results in S-tectonites, and L-S-tectonites correspond to plane strain deformations. One basic assumption, underlying these conclusions, is that the mineral grains behave entirely as passive markers. This assumes that the grain shape mimics the bulk strain of the

☐Exercise 15-2: a) Discuss the range of fabrics one may expect to find in rocks subjected to a *general prolate deformation* of $1 < K < \infty$ (see section 12-2). b) Likewise, discuss the fabrics expected for *general oblate deformations* of K-values, ranging between zero and one.

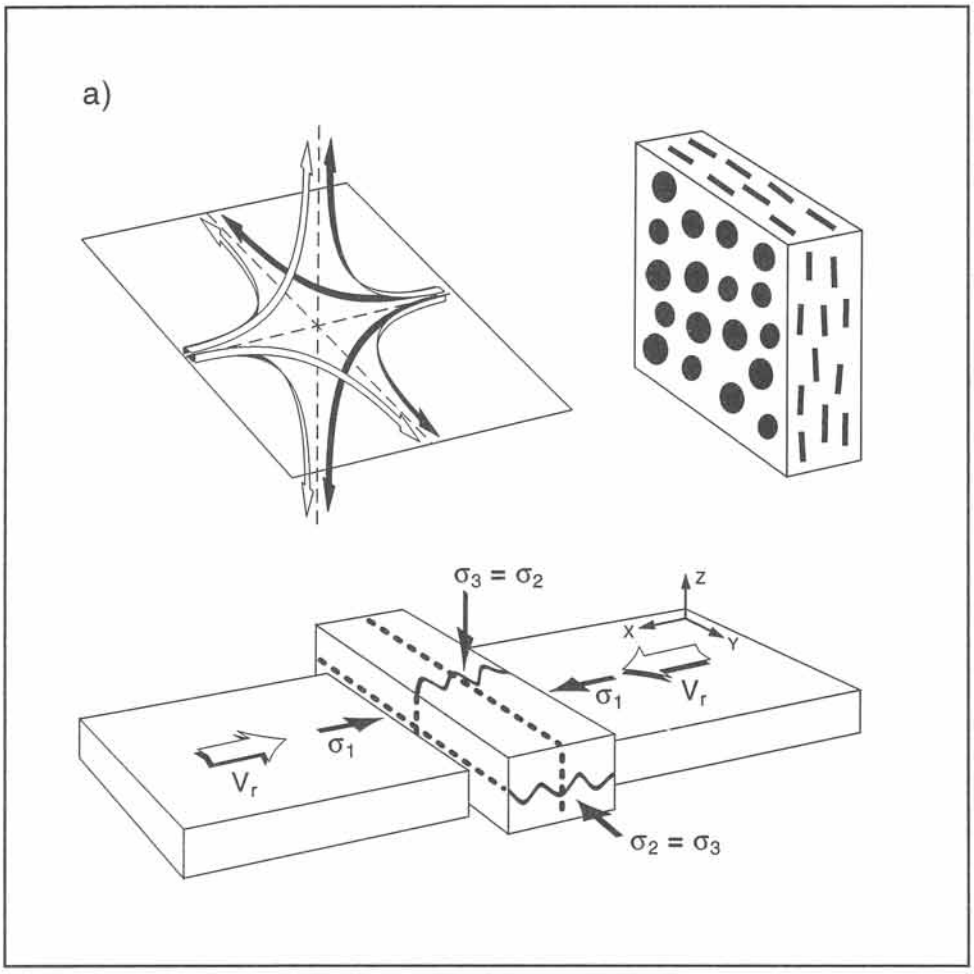

Figure 15-6a: *Streamline pattern and subvertical S-tectonite for orthogonal collision with vertical and lateral transpression. This arrangement leads to coaxial oblate deformation, extending perpendicular to shortening direction and relative velocity vector for the plates, V_R.*

rock volume of which the grain is a part. This approach is useful, but limited, because experimental grain shape studies suggest that grains are active markers and have poor strain memories; they record only part of the bulk strain.

15-3 Tectonite formation in coaxial deformation

The kinematics, leading to the different types of tectonites, can be illustrated, using a simple model of coaxial, homogeneous deformation. The development of L-, S-, and L-S-tectonites and their orientation in space can be linked to the kinematics of the wall rock of the deforming tectonites. Figure 15-5a illustrates a hypothetical bulk deformation by pure shear in an orthogonal collision zone between two rigid plates. The model concentrates on the deeper, ductile portion of the deforming crust. The displacement path of the bulk particles will outline a pure shear flow, as illustrated in the flow planes of Figure 15-5b. The particle movements are governed by the following deformation tensor:

$$\begin{bmatrix} \exp(\dot{e}_1 t) & 0 & 0 \\ 0 & \exp(\dot{e}_2 t) & 0 \\ 0 & 0 & \exp(\dot{e}_3 t) \end{bmatrix} \quad (15\text{-}1)$$

The normalized semi-axes of the finite strain ellipsoid, or principal stretches, $S_{1,2,3}$, are directly given by the diagonal elements of the deformation tensor. The relative magnitude of the stretches depends on the relative magnitude of the principal strain-rates. Progressive deformation will always be accompanied by plane strain if $\dot{e}_2$ is zero. The internal deformation may locally depart from the bulk deformation. Folding and boudinaging may occur in competent single layers, oriented as indicated in the central deformation zone of Figure 15-5a. Additionally, upright L-S-tectonites may be expected to form in plane strain between orthogonally colliding plates (Fig. 15-5c).

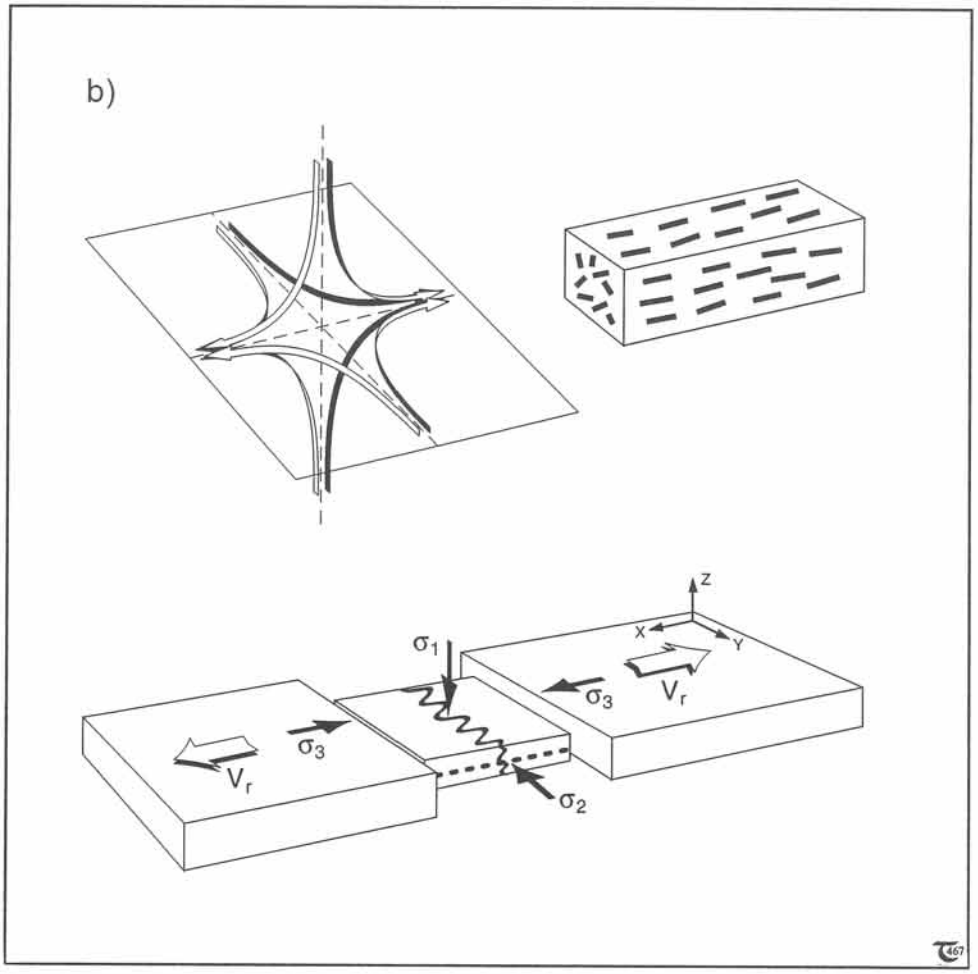

Figure 15-6b: *Streamline pattern and subvertical L-tectonite for orthogonal extension with vertical and lateral transtension (e.g., above a spreading ridge). This arrangement causes coaxial prolate deformation, aligned with the relative velocity vector for the plates, V_R.*

Figure 15-6a shows a uniaxial collision with stretching in both the vertical and lateral directions, leading to oblate strain in the deformation zone. *Subvertical* S-tectonites are formed if lateral extrusion between two colliding plates is unconstrained. The perfect oblate strain occurs if the ratio $\dot{e}_{zz}/\dot{e}_{yy}$ (or $\dot{e}_1/\dot{e}_2$) is unity, provided the strain-rates are extensional or positive. *Subhorizontal* L-tectonites may form when a crustal segment is unilaterally stretched between two diverging crustal plates (Fig. 15-6b). This situation of constrictional prolate strain arises if the ratio $\dot{e}_{zz}/\dot{e}_{yy}$ is unity, but with negative strain-rates. *Subhorizontal* S-tectonites may form in crustal sections radially expanding, such as occurs above rising plutons, gneiss domes, and buoyant salt (Fig. 15-7a). *Subvertical* L-tectonites may form in supracrustal terranes subjected to radial constriction, as occurs between encroaching plutons, within the stem of rising salt stocks, or in magma pipes (Fig. 15-7b).

☐Exercise 15-3: The various types of tectonites, here explained in terms of coaxial 3D deformation, also, can be formed in non-coaxial deformation. What type of tectonite do you expect to find in shear zones caused by simple shear?

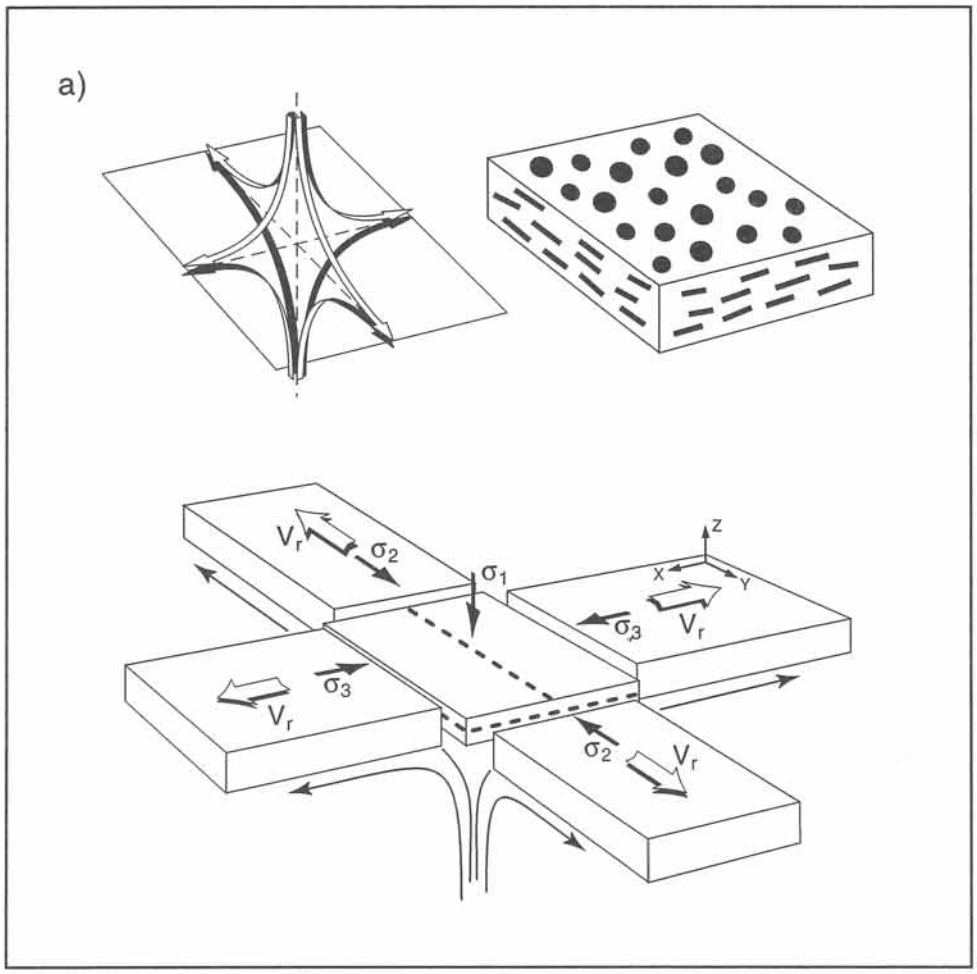

☐Exercise 15-4: Discuss ways in which the tectonites, illustrated in Figures 15-8a & b, may possibly have formed.

Figure 15-7a: *Streamline pattern and subhorizontal S-tectonite in radial extension above a ballooning pluton. This situation leads to coaxial oblate deformation.*

15-4 Determining plane strain

When strain is studied in two dimensions, it is usually assumed that no stretch occurs in the third dimension. Strain in two dimensions can be represented by a *strain ellipse* (Fig. 15-9a & b). The ellipse section studied should be perpendicular to the intermediate principal strain axis of unchanged, constant length. Study of deformation in 3D is straightforward only if the deformation is indeed confined to plane strain. If the deformation does not involve volume change, so-called *isochoric deformation*, then $S_1=1/S_3$ (cf., eq. 15-13a). The initial radius, L_0, of a spherical object, deformed by plane strain into an ellipse section with absolute principal lengths, L_1 and L_3, can be determined for strains in nature from:

$$L_0=(L_1L_3)^{1/2} \quad (15\text{-}2)$$

This follows from the definition of stretch as the normalized, deformed, semi-axial lengths, i.e., $S_1=L_1/L_0$ and $S_3=L_3/L_0$, in combination with the plane strain condition $S_1=1/S_3$. The principal stretches, S_1 and S_3, then follow directly from the absolute lengths of the semi-axes of the strain ellipse, without the need of direct knowledge of L_0:

$$S_1=(L_1/L_3)^{1/2} \quad (15\text{-}3a)$$
$$S_3=(L_3/L_1)^{1/2} \quad (15\text{-}3b)$$

The associated *axial ratio* or *ellipticity*, R_S, is as follows:

$$R_S=S_1/S_3=S_1^2 \quad (15\text{-}4)$$

The area of the principal ellipse section, A, for true plane strain and normalized by the undistorted initial circle section is:

$$A=S_1S_3 \quad (15\text{-}5)$$

The validity of the plane strain assumption can be checked by establishing that "L_0," determined from equation (15-2), is equal to L_2, as measured on the sample.

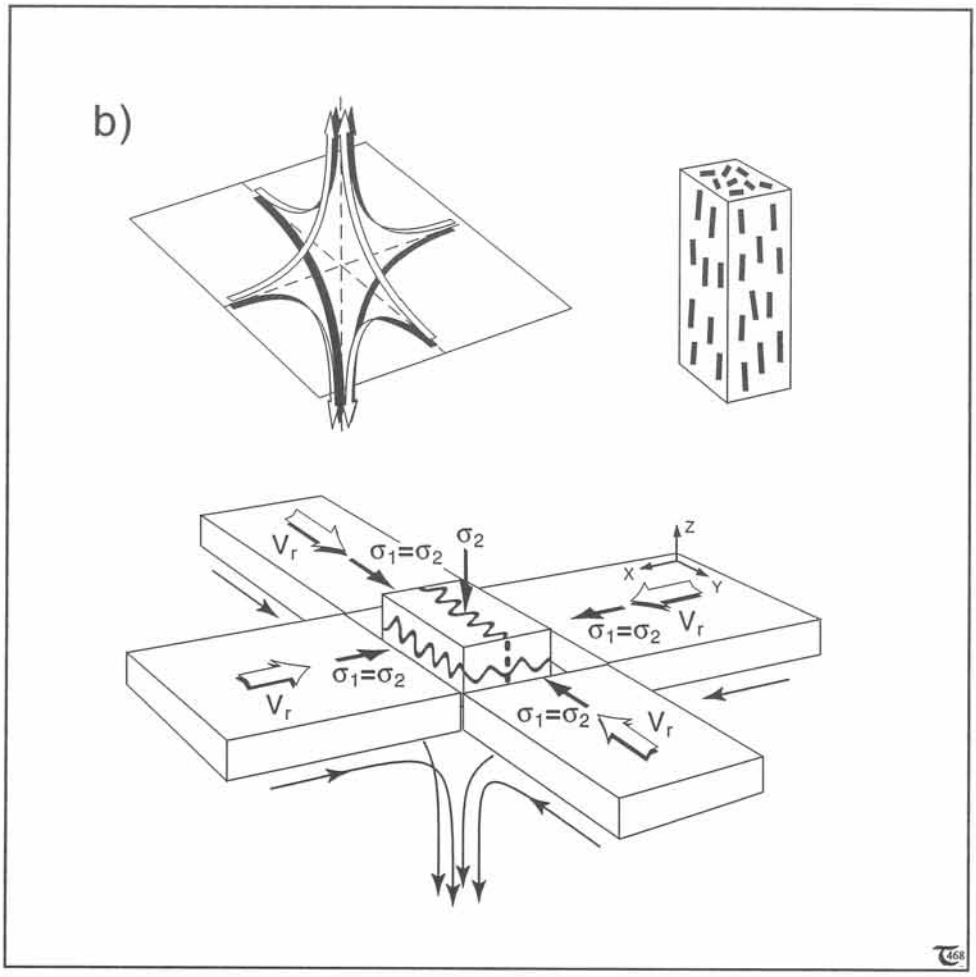

Figure 15-7b: *Streamline pattern and subvertical L-tectonite in supracrustal sink flow between buoyant plutons (or within a rising salt dome), leading to coaxial prolate deformation.*

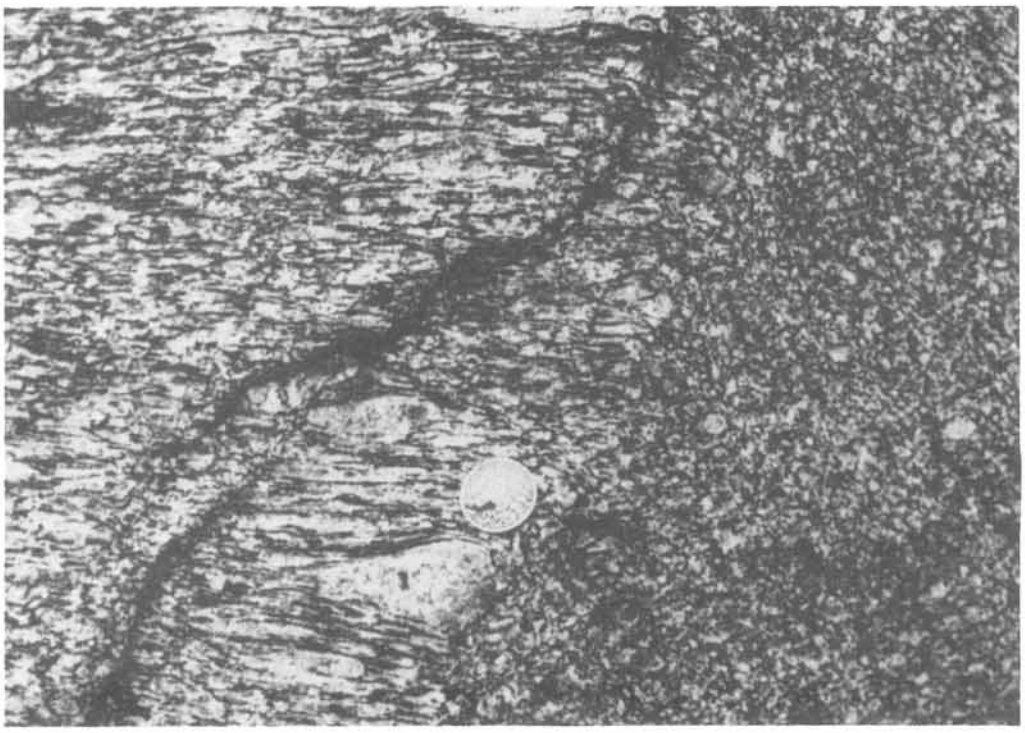

Figure 15-8a: *Gneissic tectonite outcrop, referred to in exercise 15-4. Courtesy John Ramsay.*

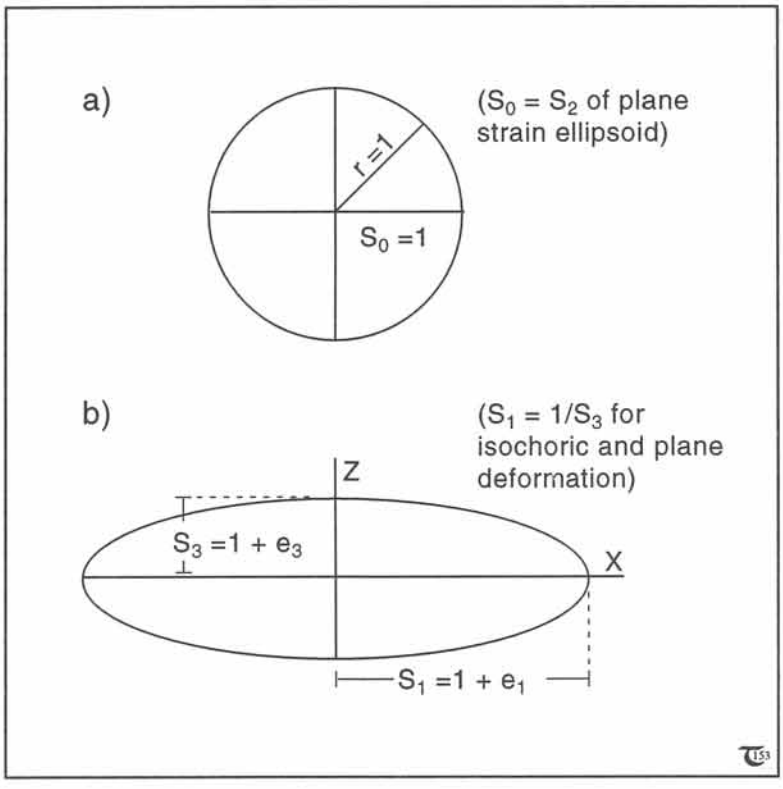

Figure 15-9: *a) & b) Undeformed strain circle and deformed strain ellipse for plane strain. The principal semi-axes are normalized, using their actual dimensional lengths, according to expressions (15-3a & b).*

Figure 15-8b: Amphibolite gneiss, referred to in exercise 15-4.

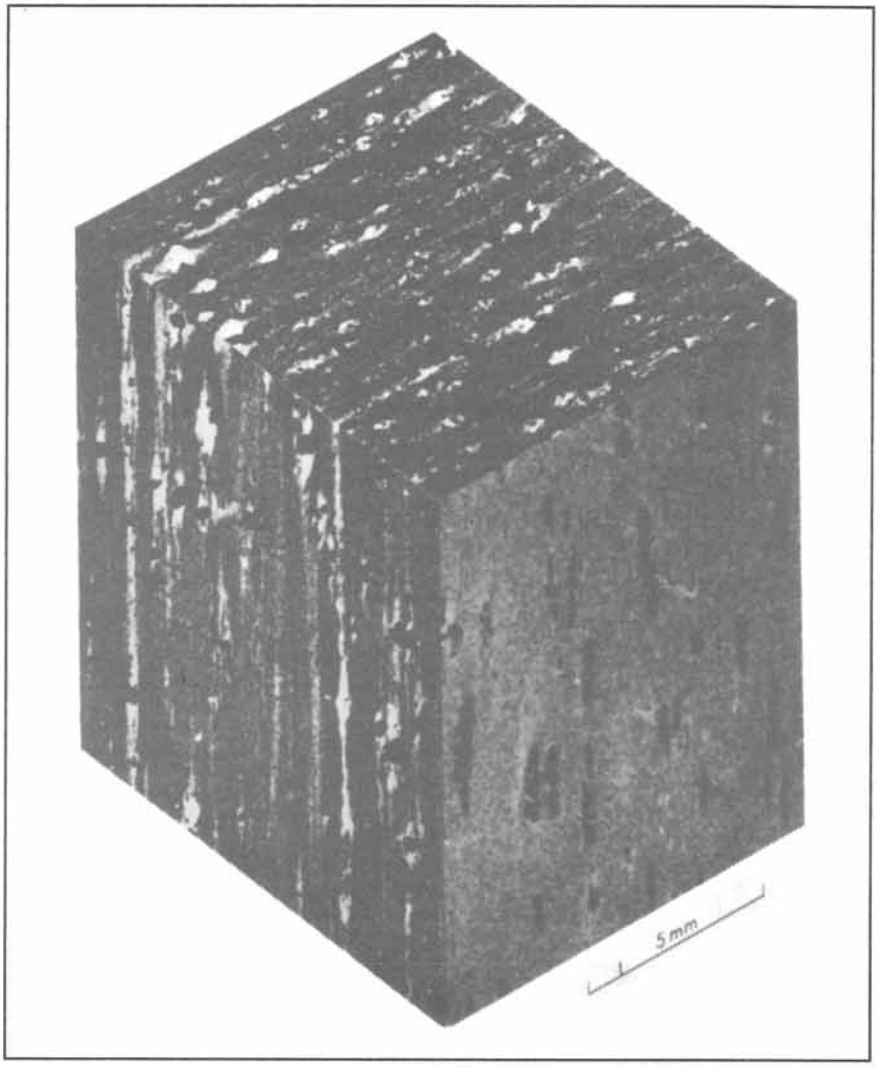

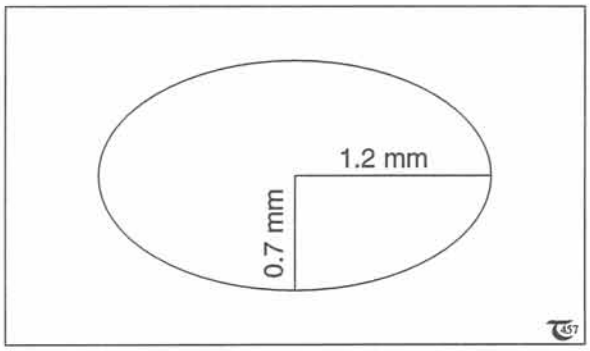

Figure 15-10: Deformed ooid with dimensional semi-axial lengths, as indicated. See exercise 15-5.

□Exercise 15-5: Figure 15-10 illustrates a section through a material ellipsoid, outlined by a deformed ooid. The section shown contains the long and the short axis of the material ellipsoid. a) Assuming plane strain and no volume change, what must be the *absolute length*, L_2, of the intermediate axis of the material ellipsoid (perpendicular to the plane of view)? What is the magnitude of the *stretch*, S_2? b) Determine the value of stretches S_1 and S_3. c) Determine the ellipticity, R. d) Determine both the *absolute area* and *normalized area* of the ellipse section.

15-5 Determining isochoric non-plane strains

Deformations involving no volume change are termed *isochoric*. The initial radius, L_0, of any spherical object, *isochorically* deformed into either a prolate or oblate ellipsoid of semi-axial lengths, L_1, L_2, and L_3, is:

$$L_0=(L_1L_2L_3)^{1/3} \qquad (15\text{-}6)$$

The stretches for a general isochoric 3D deformation follow from the absolute lengths of the semi-axes of the observed ellipsoid sections:

$$S_1=L_1^{2/3}/(L_2L_3)^{1/3} \qquad (15\text{-}7a)$$
$$S_2=L_2^{2/3}/(L_1L_3)^{1/3} \qquad (15\text{-}7b)$$
$$S_3=L_3^{2/3}/(L_2L_1)^{1/3} \qquad (15\text{-}7c)$$

The normalized area of the principal ellipse section, A (normalized by the unit area of the intial sphere section), is:

$$A=S_1S_3=(L_1L_3)^{1/3}/L_2^{2/3} \qquad (15\text{-}8)$$

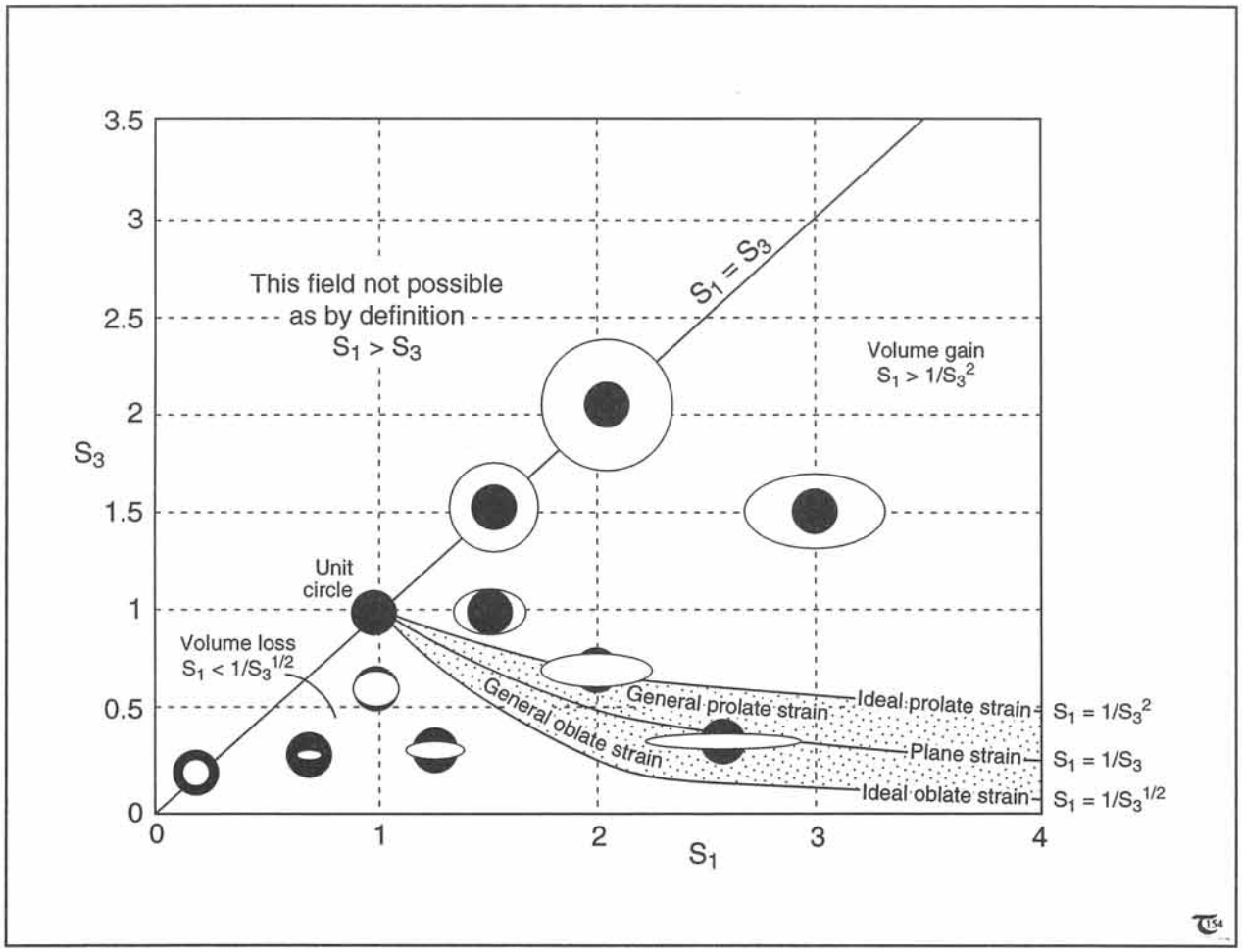

Figure 15-11: *Plot of S_1 versus S_3. Distinguished are the line for volume changes without strain ($S_1=S_3$), and curves for plane strain ($S_1=1/S_3$), ideal prolate strain ($S_1=1/S_3^2$), and ideal oblate strain ($S_1=1/S_3^{1/2}$). The field of general prolate strain occurs for $(1/S_3)<S_1<(1/S_3)^2$ and that of general oblate strain occurs for $(1/S_3)>S_1>(1/S_3)^{1/2}$, both without volume change. Deformations, accompanied by volume gain and loss, occur for $S_1>(1/S_3^2)$ and $S_1<(1/S_3^{1/2})$.*

It follows that, if S_1 and S_3 are overestimated by neglecting any shortening of S_2, due to usage of equations (15-3a & b) rather than (15-7a & c), the normalized area, A, will appear larger than unity. Conversely, if S_1 and S_3 are underestimated by neglecting any extension of S_2, due to usage of equations (15-3a & b) rather than (15-7a & c), the normalized area, A, will appear smaller than unity.

☐Exercise 15-6: Refer to exercise 15-5. a) If measurement of L_2 would now indicate a real stretch, S_2, of 1.2, what would be the normalized area of the (S_1,S_3)-strain ellipse section? b) What is the shape of the strain elllipsoid, prolate or oblate?

☐Exercise 15-7: Derive equation (15-6), using the definition of the stretches and the condition of no volume change.

15-6 Determining volume changes

If strains are studied in 3D, the concept of the strain *ellipse* is expanded into an *ellipsoid* of unit volume. The introduction of the strain ellipsoid provides a tool to discuss the possible involvement of any volume change during the deformation of rocks. Consider a plane strain, which initially assumed L_2 was left unchanged by the deformation. If it later turns out that "L_0," determined from equation (15-2) is larger than the measured L_2, then the sectional area of the (S_1, S_3)-ellipse must have increased by shortening of L_2, during the deformation. The strain ellipsoid will approach a prolate shape, and it, thus, departs from the plane strain shape that was initially assumed for practical convenience. Strain ellipses (S_1,S_3-sections), involving increase or decrease in sectional area, can be visualized by plotting S_1 versus S_3 (Fig. 15-11). The curve for plane strain ellipses is defined by:

$$S_1 = 1/S_3 \qquad (15\text{-}9a)$$

because $S_1S_2S_3 = 1$ and $S_2 = 1$ (Fig. 12-2b). Perfect

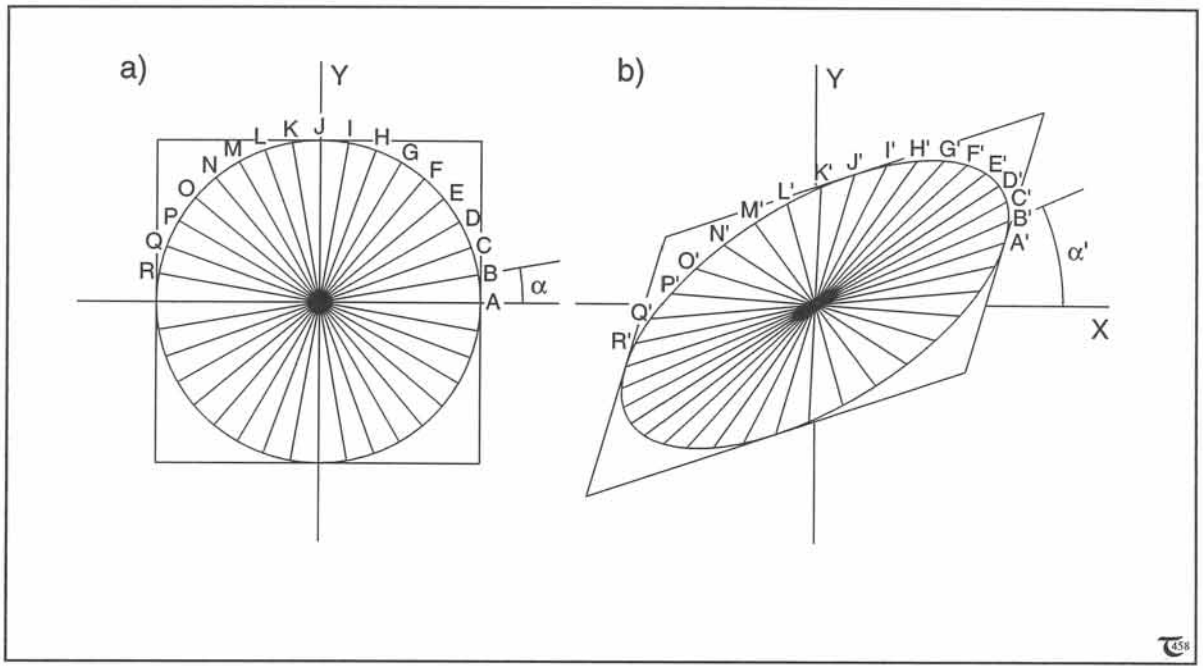

Figure 15-12: a) & b) Undeformed strain circle and deformed ellipse for a general plane strain. Equally spaced lines in the undeformed state rotate at different rates during deformation.

isochoric, prolate strains have:

$$S_1 = 1/S_3^2 \qquad (15\text{-}9b)$$

because $S_1S_2S_3 = 1$ and $S_2 = S_3$ (Fig. 12-2c). Perfect *isochoric*, oblate strains have:

$$S_1 = 1/S_3^{1/2} \qquad (15\text{-}9c)$$

because $S_1S_2S_3 = 1$ and $S_2 = S_1$ (Fig. 12-2d).

It folllows from the above relationships that true volume gain must have occurred if $S_1 > 1/S_3^2$. Maximum volume gain may occur when $S_1 = S_3$, and is limited by the definition $S_1 \geq S_3$. Likewise, true volume loss must have occurred if $S_1 < 1/S_3^{1/2}$, and maximum volume decrease occurs when $S_1 = S_3$, and is limited by the definition $S_1 \geq S_3$.

☐Exercise 15-8: Use the stretches values of cases (a) to (c) in exercise 12-1 to check the validity of equations (15-9a to c).

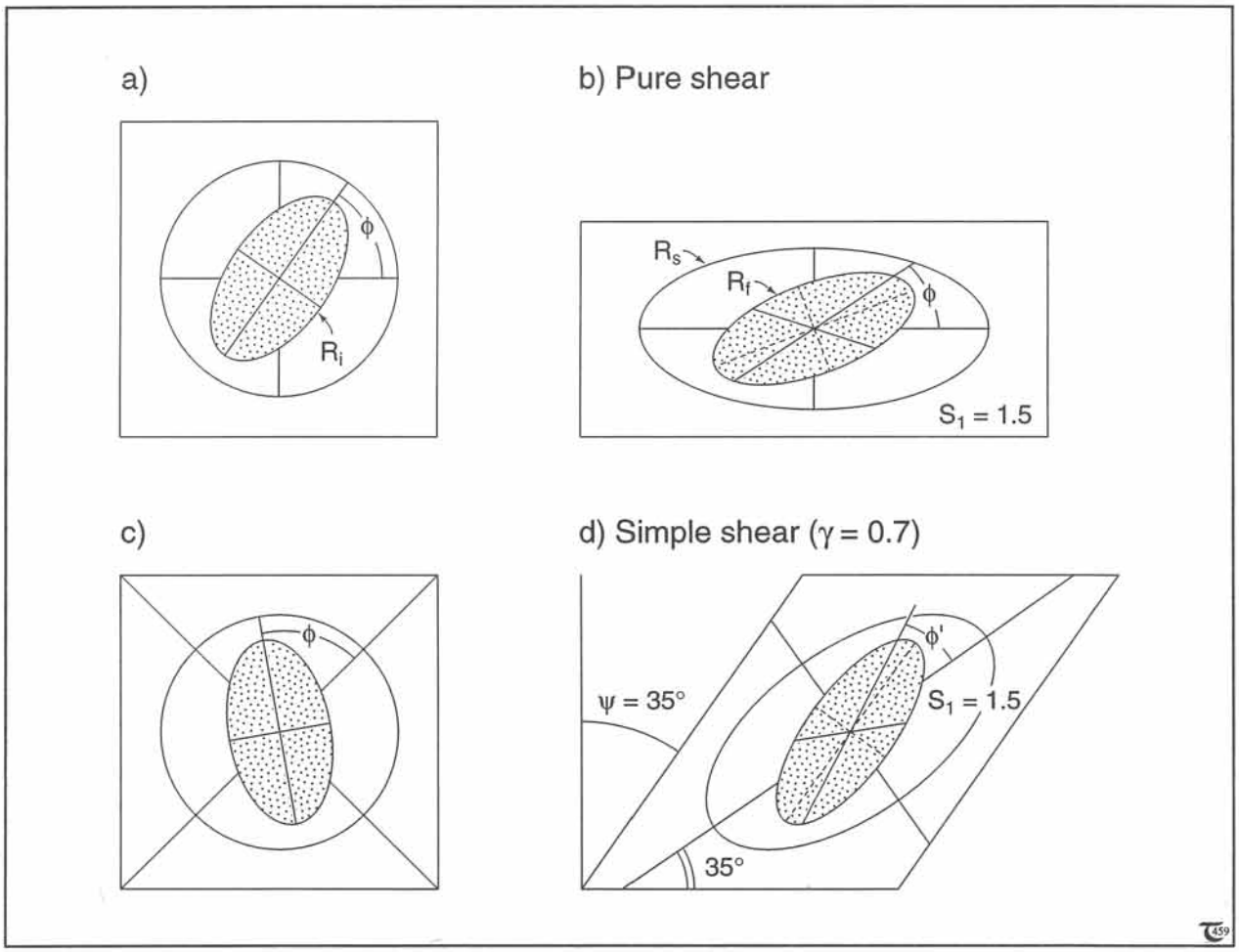

Figure 15-13: *a) to d) Deformation of elliptical objects by pure shear (a & b) and simple shear (c & d). For this case the initial orientation of the elliptical object and amount and direction of deformation are chosen such that similar strain ellipses result.*

15-7 (R_f,ϕ)-method for elliptical objects

Figures 15-12a & b illustrate a general homogeneous deformation of an initially circular object. It is important to realize that, after deformation, straight lines remain straight, parallel lines remain parallel and have similar stretches, the angles between lines are changed, and circles are transformed into ellipses.

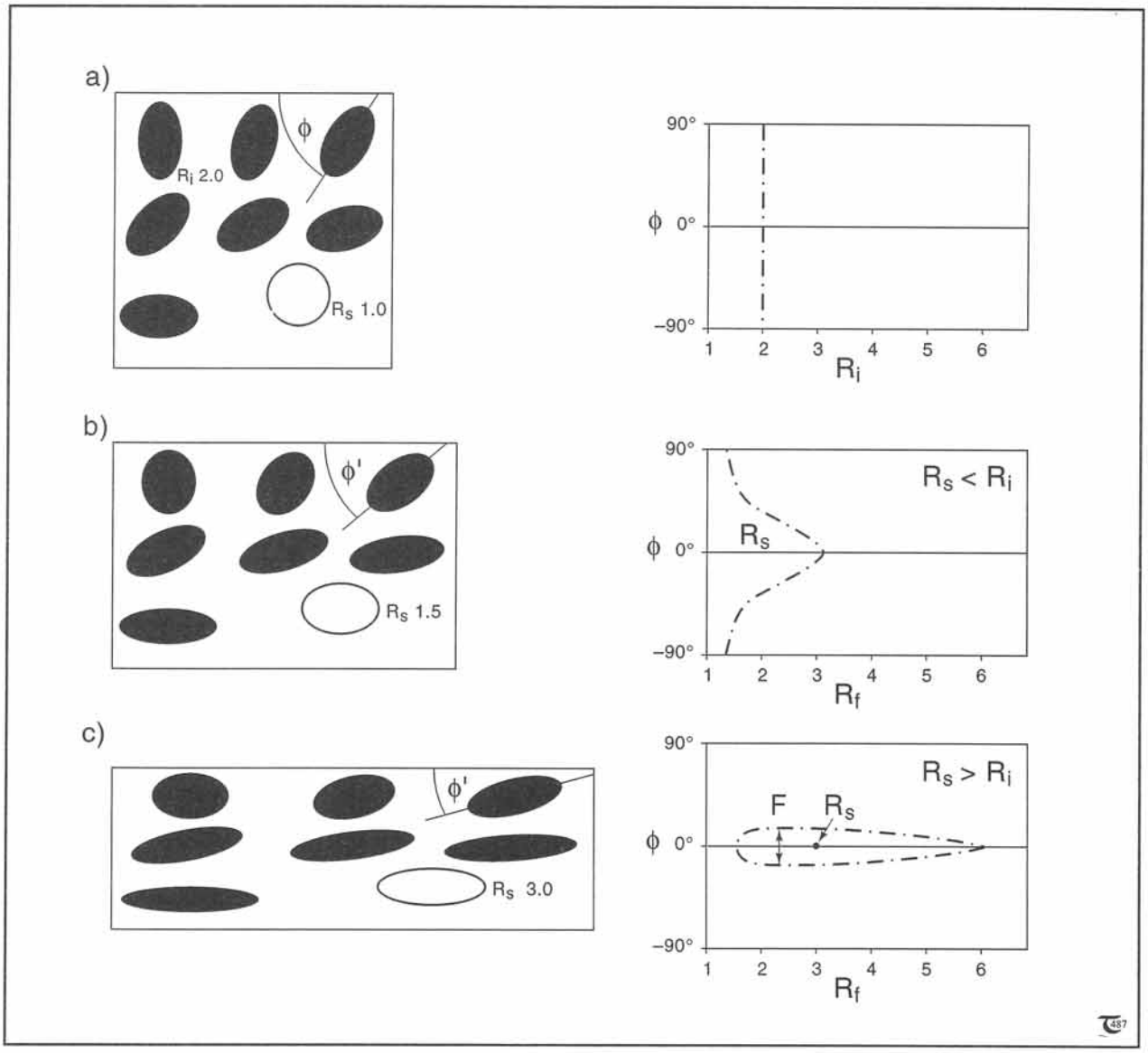

Figure 15-14: *a) Randomly oriented elliptical objects in undeformed volume and corresponding (R_i,ϕ)-plot. The straight line plotted gives the initial ellipticity of the objects, which is uniform in this case. b) Appearance of hypothetical rock fabric after bulk finite strain, R_s, of 1.5 superposed on that of (a). The finite strain, R_s, follows from the lowest R_f, as indicated in the (R_f,ϕ)-plot. c) Similar fabric after bulk strain, R_s, of 3. The (R_f,ϕ)-plot shows a typical tear drop curve, which appears only if $R_s > R_i$. The actual value of R_s follows from equation (15-10a). The value of R_i follows from equation (15-10b).*

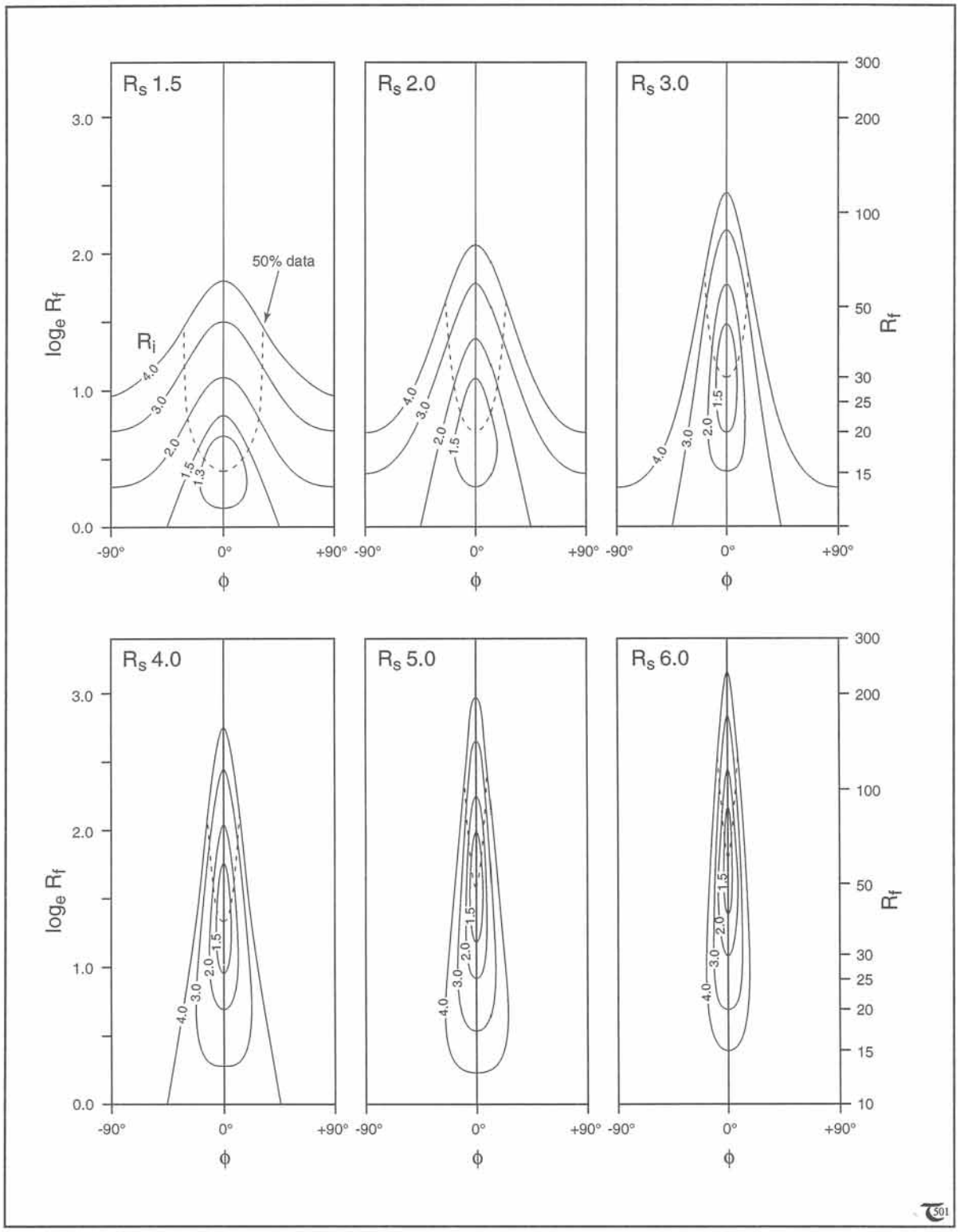

Figure 15-15: *Standard (R_f,ϕ)-plots for finite strain (R_s) of 1.5, 2, 3, 4, 5, and 6. The family of (R_f,ϕ)-curves in each plot arises if populations of different initial ellipticities (R_i) occur.*

Practical strain measurements have established that very few rocks contain strain markers of initial spherical shape. Even undeformed ooids may deviate from the spherical shape so much that they can be considered better as initially ellipsoidal objects. Figures 15-13a to d demonstrate that objects, originally of elliptical shape, deform into ellipses of different orientation and aspect ratio. The ellipticities of each of three ellipses (initial object, R_i, final object, R_f, and strain ellipse, R_s) generally are all different. The axial ratio of the deformed ellipse, R_f, may be larger or smaller than that of the initial ellipse, R_i, depending upon the orientation of the stretching directions. The orientations of the initial elliptical objects, the deformed elliptical objects, and the finite strain ellipses are all likely to be different.

Both the final orientation, ϕ, and the ellipticity, R_f, of deformed elliptical objects depend on the angle the elliptical objects made initially with the stretching directions. In practical applications, the ellipticity, R_f, of the deformed objects is plotted against ϕ. The ellipticity of the finite strain, R_s, can be estimated, according to this so-called (R_f,ϕ)-method. The method assumes that the elliptical objects were initially oriented randomly (but all having their principal plane coinciding with the plane of section). Figure 15-14a illustrates the undistorted ellipses and a plot of the initial ellipticity of the objects, R_i, against their orientation, ϕ, with respect to an arbitrary reference line. The (R_f,ϕ)-plot of the undeformed rock will be a straight line, provided the initial ellipticity of the objects, R_i, is uniform. The ellipticity of initial objects is likely to vary, and this can be accounted for in the (R_f,ϕ)-method (see below).

Figure 15-14b illustrates a finite strain ellipticity, R_s, of 1.5 and the corresponding pattern of the (R_f,ϕ)-plot. The peak in the (R_f,ϕ)-plot gives an ellipticity for R_f of 3. The finite strain ellipticity, R_s, of 1.5 follows directly from the lower R_f-values, as indicated in Figure 15-14b. A larger finite strain with ellipticity, R_s, of 3, illustrated in Figure 15-14c, constrains the spread in orientation (or fluctuation, F) of ϕ and results in a typical teardrop-shaped curve. The teardrop curve arises only if the strain ellipse has an ellipticity larger than that of the initial elliptical objects ($R_s > R_i$). The values of R_s and R_i then are as follows:

$$R_s = (R_{f\,max}\, R_{f\,min})^{1/2} \qquad (15\text{-}10a)$$

$$R_i = (R_{f\,max}/R_{f\,min})^{1/2} \qquad (15\text{-}10b)$$

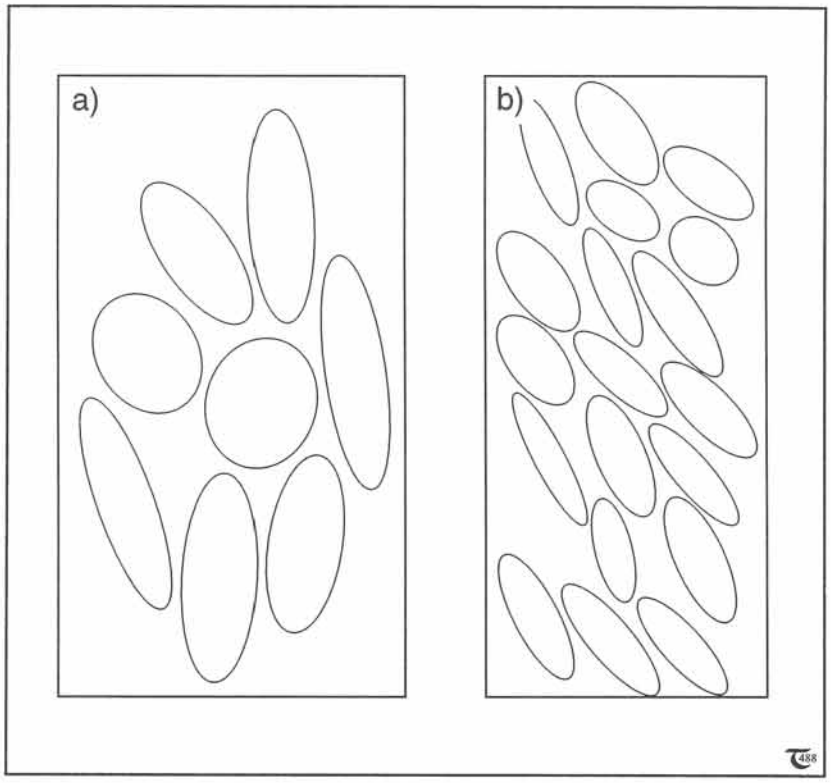

Figure 15-16: *a) & b) Tracings of deformed pebbles in deformed conglomerate. The sections contain the major and minor principal lengths, L_1 and L_3, of the material ellipsoids outlined by the deformed pebbles. The ellipticity is $R_f = L_1/L_3$. See exercise 15-9.*

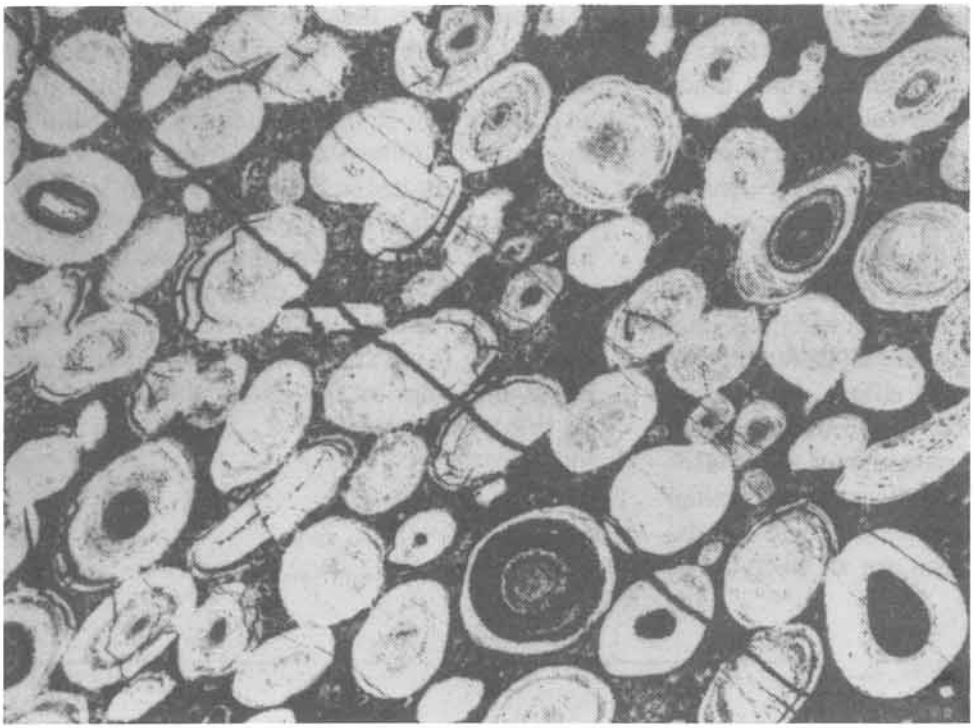

□Exercise 15-9: Construct (R_f,ϕ)-plots for each of the three outcrop tracings in Figure 15-16a to c. Determine the values of R_S, R_i, and the orientation of S_1 for each case.

Figure 15-16c: *Thin section micrograph of deformed oolitic limestone. See exercise 15-9. Courtesy John Ramsay.*

If the initial ellipticities of the objects, R_i, are both variable and larger than R_S, then the (R_f,ϕ)-plot may show as a diffuse field of dots. The finite strain of the rock is then best established by comparing the (R_f,ϕ)-plot for your particular case with theoretical plots, such as shown in Figure 15-15. [(R_f,ϕ)-charts are found in Lisle, 1988.]

15-8 Stretched-line method for linear objects

Many bedding planes may expose deformed stretched belemnites, crinoids, crystals, or single layers. Figure 15-17 sketches two stretched belemnites within a plane with a clear stretching or extension lineation. Belemnites are the remnants of marine encephalopods (squids), found in Jurassic and Cretaceous sedimentary rocks. They are made up of crystalline calcite fibers and are commonly more brittle than the surrounding marls and marly limestones in which they occur. The belemnites breakup into separate fragments when stretched, and their initial length, L_0, can be reconstructed by summing up the lengths of the individual fragments. The spaces between the fragments are commonly filled with fibrous quartz or calcite.

The extension lineation in Figure 15-17 is most likely parallel to the direction of greatest extension or the S_1-axis. The stretch of the belemnite, S_x, follows from $S_x=L_x/L_0$. The principal stretch, S_1, follows from the following equation [see section 14-2 and equation (14-1)]:

$$S_\phi=[S_1^2\cos^2\phi'+(1/S_1)^2\sin^2\phi']^{1/2} \qquad (15\text{-}11)$$

for plane strain. The angle, ϕ', is measured between the belemnite and the S_1-direction. The stretch, S_ϕ, here is equal to S_x.

If the deformation was not by plane strain, two stretched lines are needed for the strain analysis (because the theorem $S_1=S_3^{-1}$ no longer holds):

Figure 15-17: Sketch of stretched belemnites in L-S tectonite. See exercise 15-10.

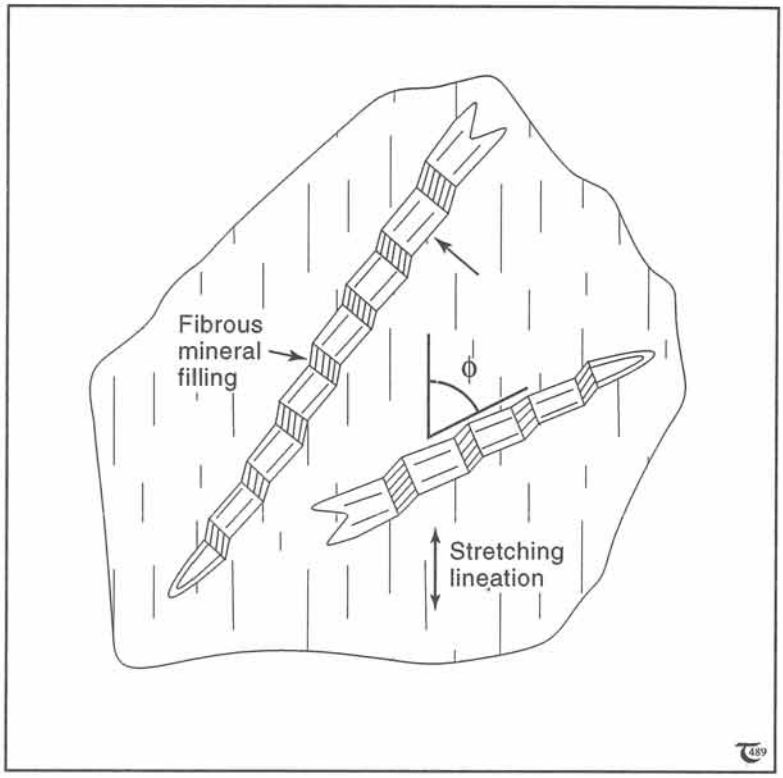

$$S_\alpha = (S_1^2\cos^2\alpha + S_3^2\sin^2\alpha)^{1/2} \quad (15\text{-}12a)$$
$$S_\beta = (S_1^2\cos^2\beta + S_3^2\sin^2\beta)^{1/2} \quad (15\text{-}12b)$$

The stretches, S_α and S_β, are for each of the linear objects used, and α and β are the respective angles with the S_1-directions outlined by the stretching lineation.

□Exercise 15-10: Examine the two stretched belemnites in Figure 15-17, and establish whether the deformation was by plane strain or not. Establish S_1, S_3, and R_S, using the graph of Figure 14-6c.

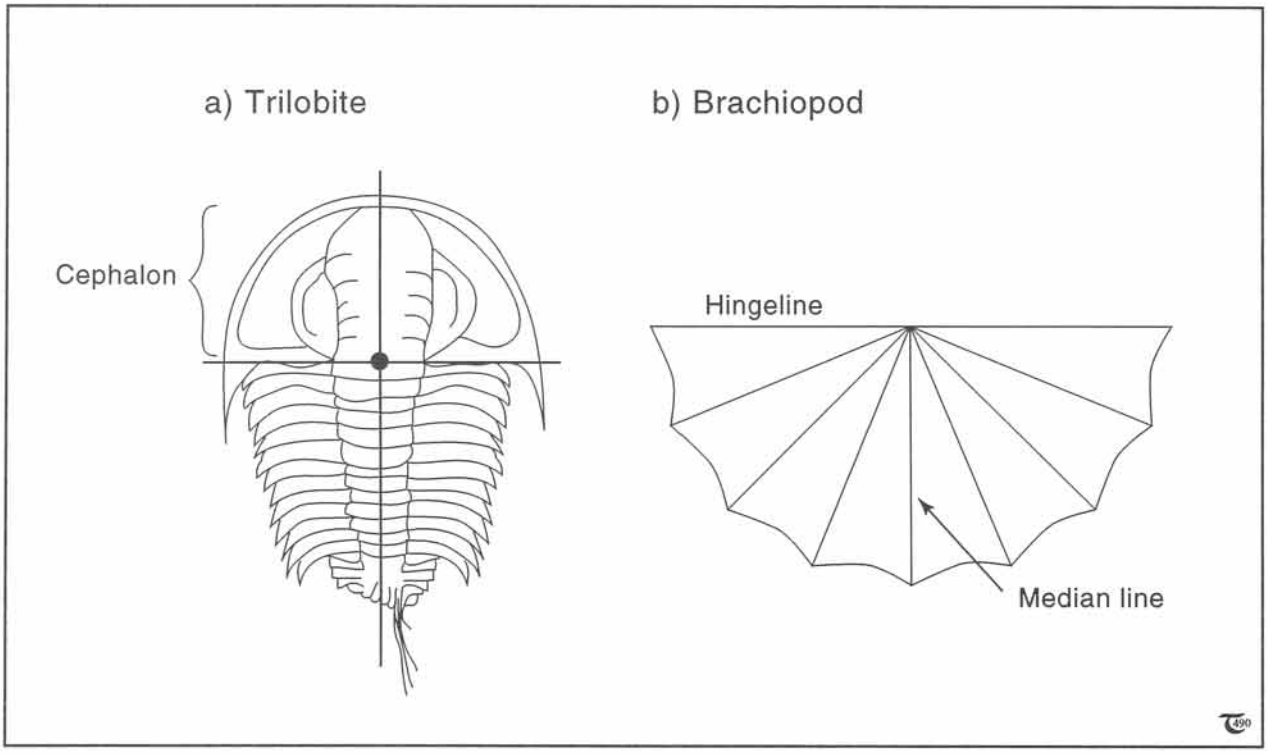

Figure 15-18: a) & b) Two examples of fossil specimens with bilateral symmetry, suitable for strain analysis by either the Wellman or Breddin method if the specimens are from deformed rocks.

15-9 Wellman and Breddin methods for angular objects

Undeformed fossils sometimes possess bilateral symmetry, so that the initial angle between, at least, two linear features is known. Figures 15-18a & b illustrate a trilobite and a brachiopod, each having lines perpendicular to the line of bilateral symmetry. For the brachiopod, the median line is normal to the symmetry line; for the trilobite, the division between the cephalon and the rear body is normal to the symmetry line. The two principal techniques considered in turn below are the Wellman method and the Breddin method.

The *Wellman method* is a quick graphical technique to obtain the strain ellipse from a population of, at least, ten differently oriented fossils of formerly bilateral symmetry. A photograph or surface tracing of the plane, containing the deformed fossils, is used as a starting point. Figures 15-19a & b explain the theoretical basis of the technique. The set of perpendicular lines of the undeformed fossil can be translated parallel to themselves to form triangles about a line, AB, of arbitrary length and orientation. A multitude of differently oriented fossils thus plotted would trace the undeformed unit circle. Figure 15-19b applies the same principle to the deformed lines,

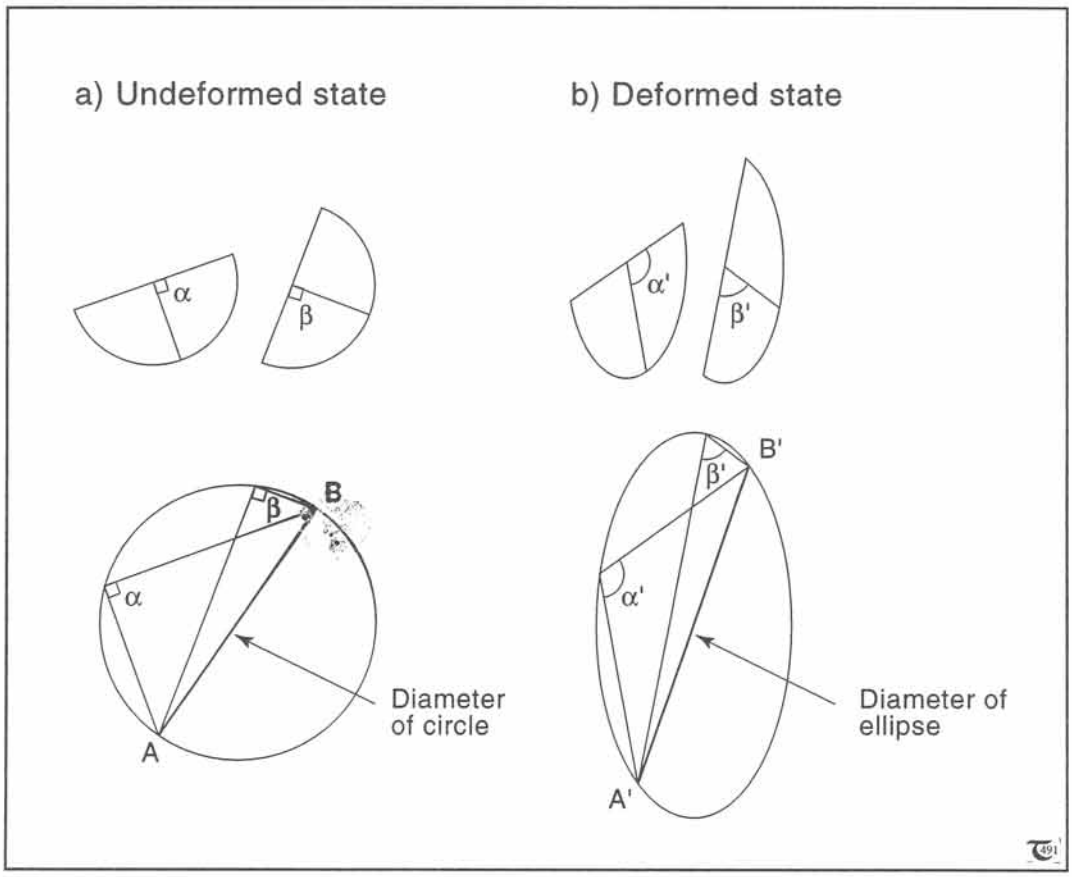

Figure 15-19: *a) & b) Wellman technique for strain analysis draws a line, AB, of arbitrary length and orientation. Line AB then acts as the base of triangles, constructed by translating parallel to themselves systematic sets of lines in fossils, either deformed (b) or undeformed (a).*

and it follows that these trace the strain ellipse. Figures 15-20a to c illustrates many differently oriented brachiopods and the steps involved to obtain the strain-ellipse shape, according to the Wellman technique.

☐Exercise 15-11: Use the Wellman-method to determine the shape and orientation of the strain ellipse from the deformed fossils for the two different localities illustrated in Figures 15-21a & b.

The *Breddin method* can be used to obtain the strain ellipse from one deformed (initially bilaterally symmetric) fossil only, provided the direction of maximum extension, S_1, is known. The starting point is an equation, which relates the two principal stretches to the angular distortion, ψ, and the angle, θ', measured between S_1 and the extended fossil line (Figs. 15-22a & b):

$$R_s = S_1/S_3 = [\tan(\theta' + \psi)/\tan\theta']^{1/2} \qquad (15\text{-}13)$$

This relationship is graphed in Figure 15-22c. This graph or equation (15-13) allows the estimation of the strain ellipticity, R_s, from a deformed fossil specimen.

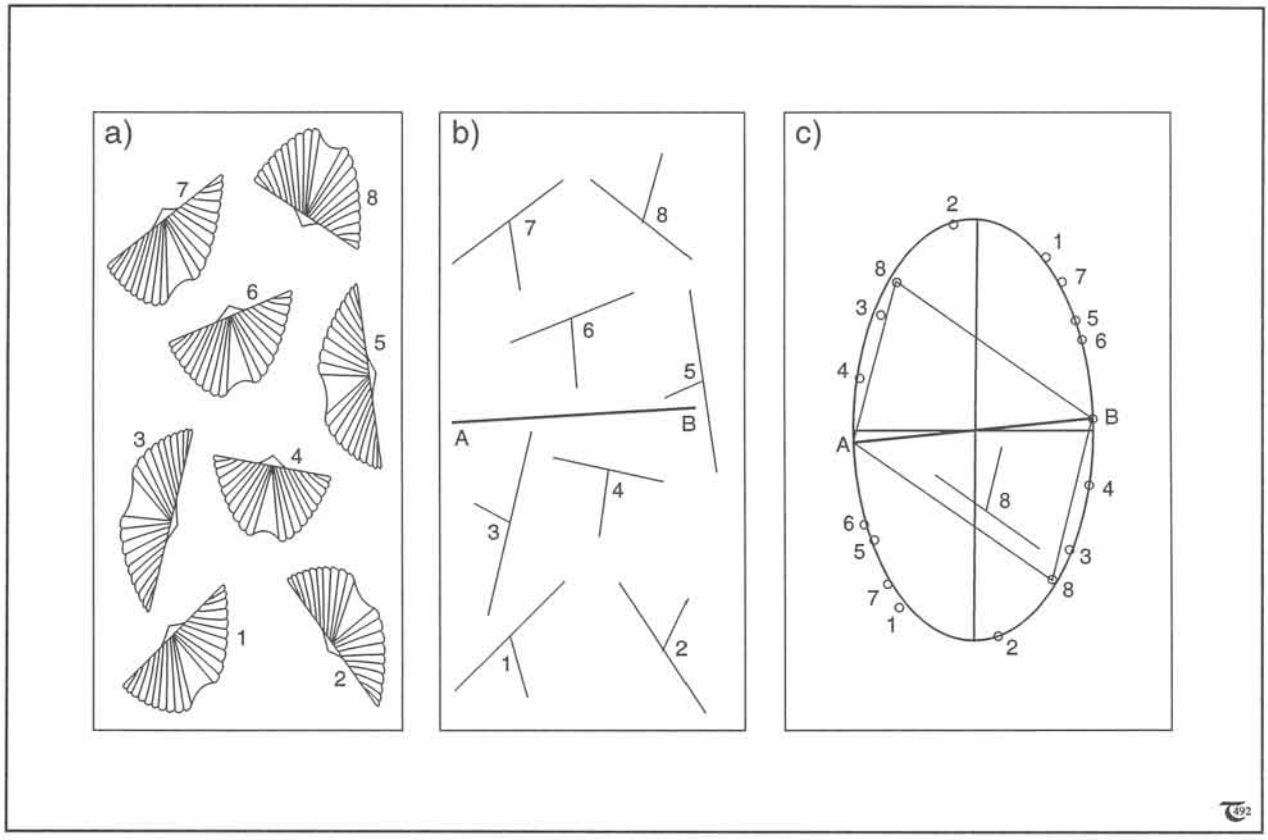

Figure 15-20: *a) to c) Theoretical basis of Wellman strain-ellipse construction: (a) Random set of deformed brachiopods photographed from outcrop. (b) Tracings of the hingelines and median lines of the brachiopods. (c) Wellman plot for the data set seen in (b). The finite strain ellipse is estimated by a best fit of the triangle points labelled 1 to 8.*

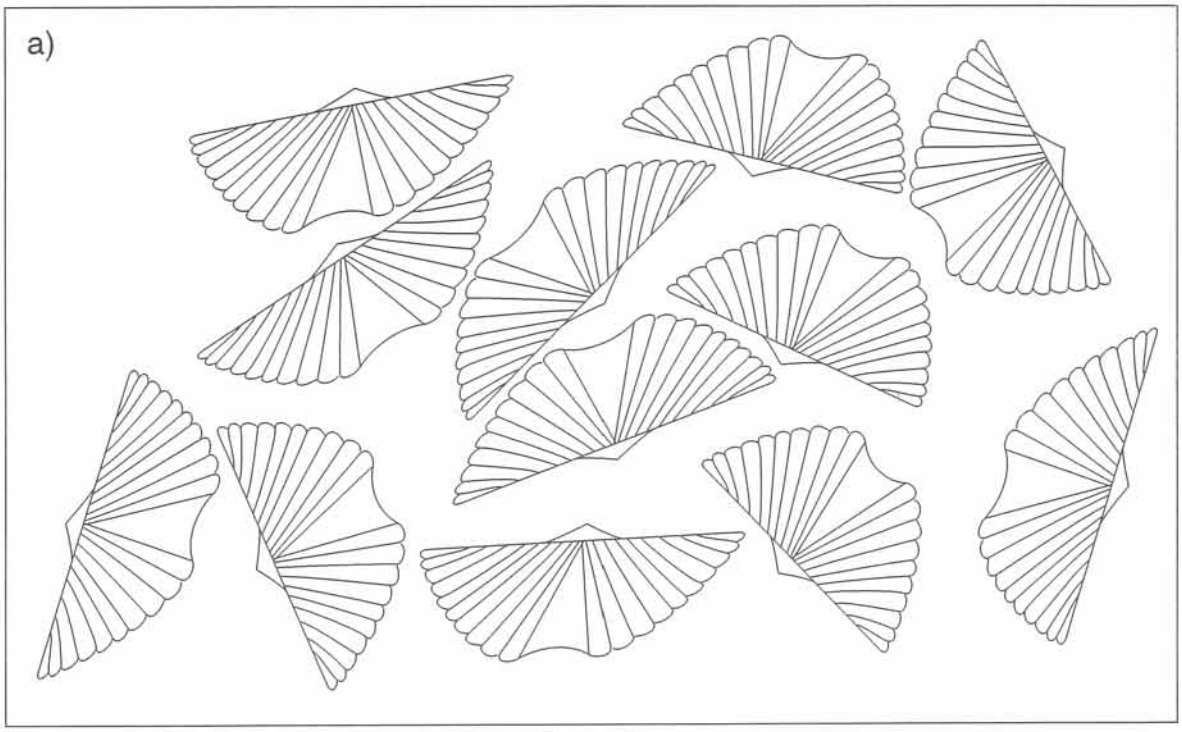

Figure 15-21a: *Deformed states of initially bilaterally symmetric brachiopods.*

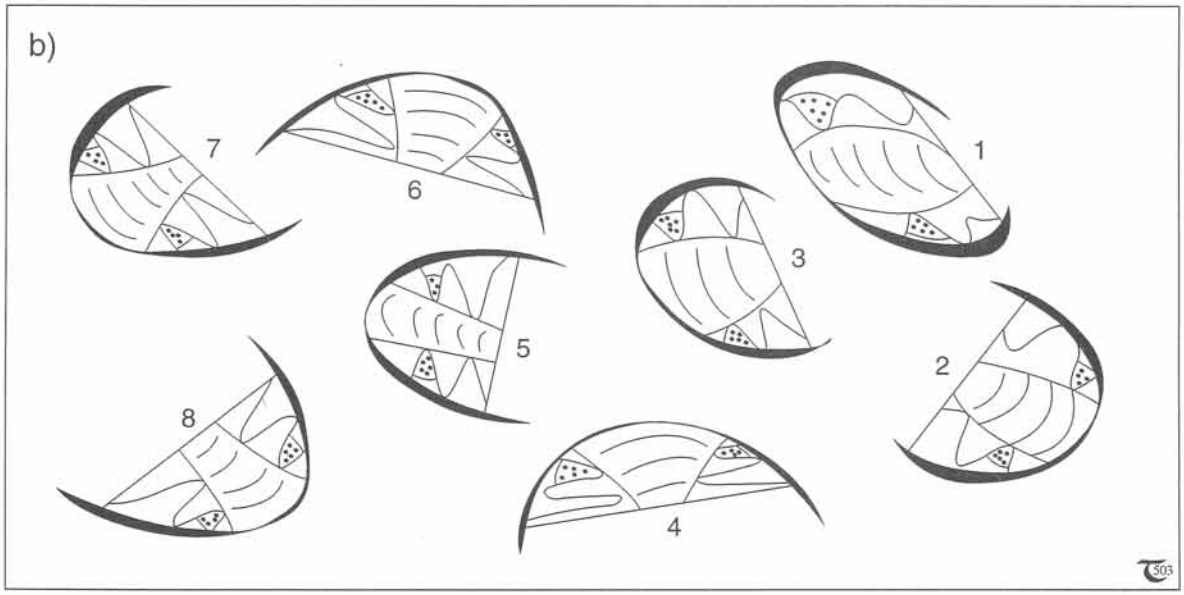

Figure 15-21b: *Deformed states of initially bilaterally symmetric cephalons of trilobites.*

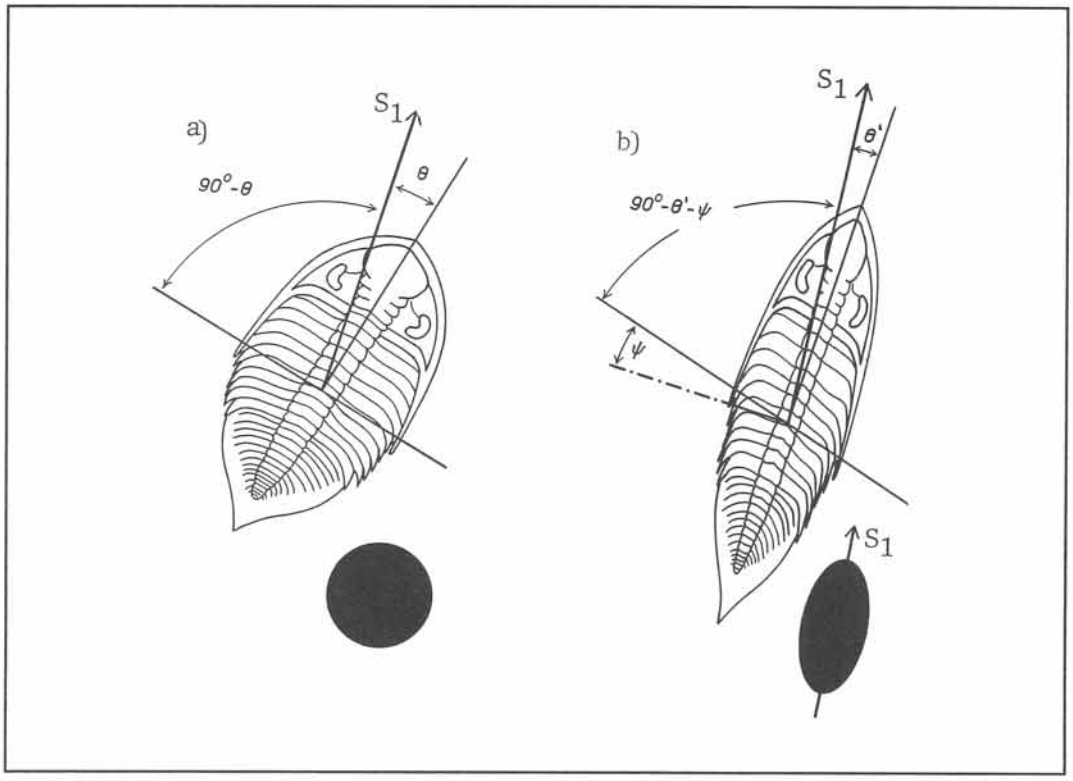

Figure 15-22a & b: *Undeformed and deformed states of initially bilaterally symmetric fossil.*

☐**Exercise 15-12: Use the Breddin method to establish the shape and orientation of the strain ellipse from the deformed trilobite specimens for the two different localities illustrated in Figures 15-23a and b.**

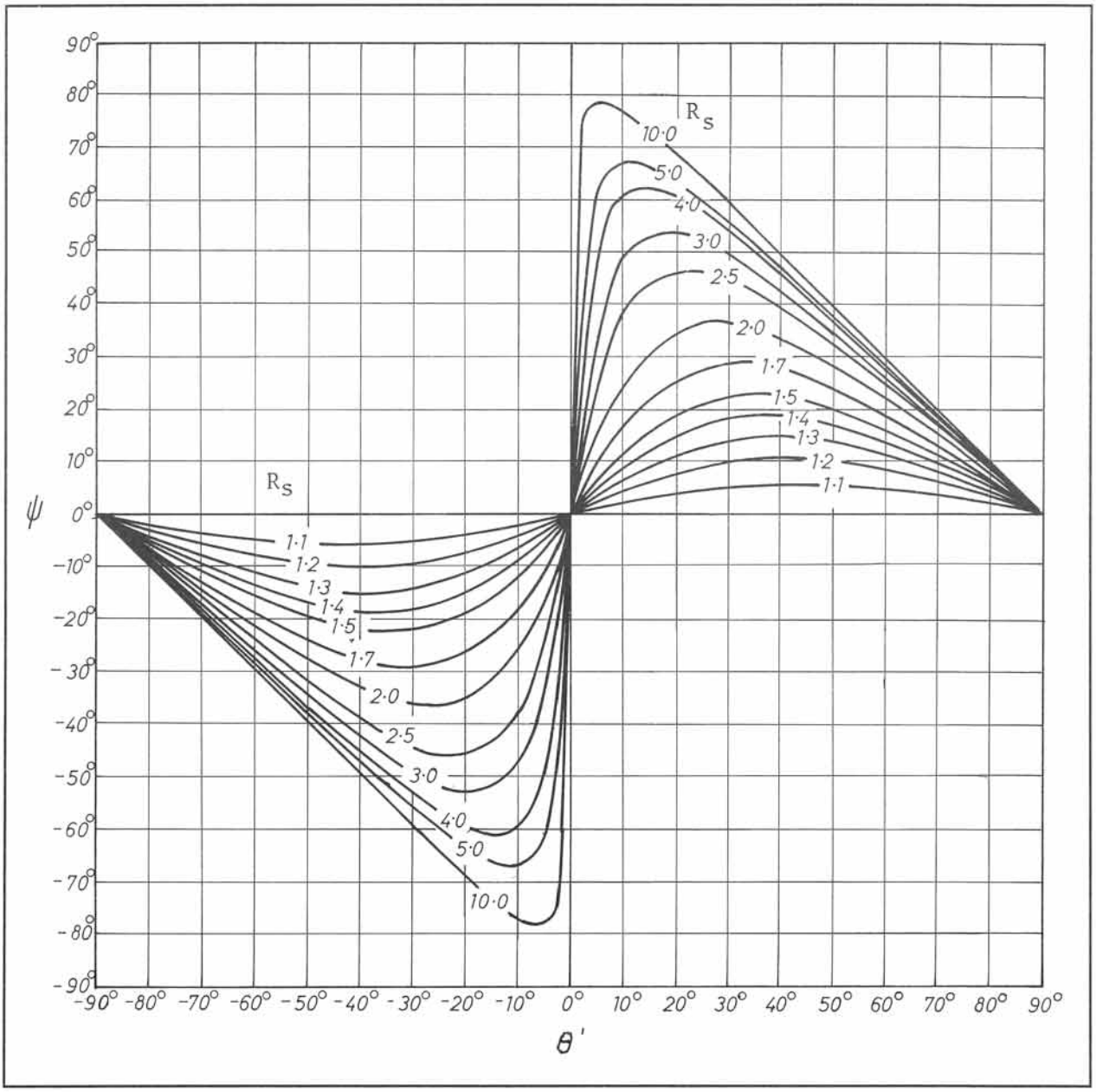

Figure 15-22c: *Breddin curves, generated by plotting angular distortion, ψ, versus orientation, θ' (see Figure 15-21b) for a range of finite strains, R_s, using equation (15-13). See exercise 15-12.*

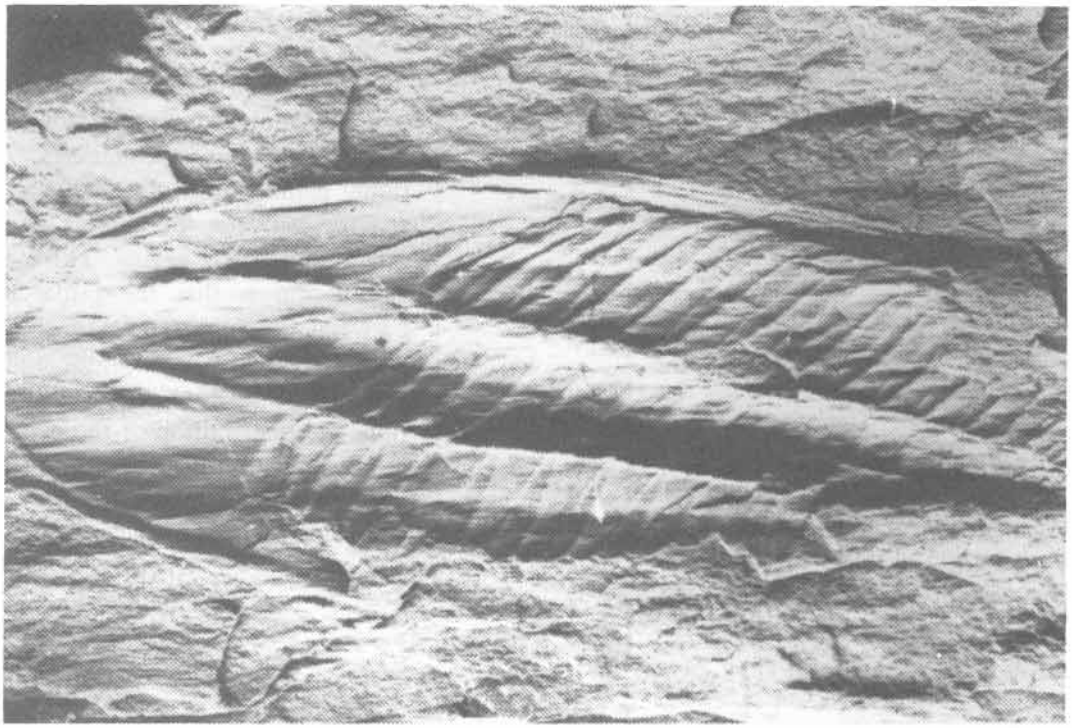

Figure 15-23: *a) & b) Examples of deformed Ordovician Angelina trilobites, originally bilaterally symmetric. The extension lineation, marked by the shadow striations, is assumed to coincide with the S_1-direction. See exercise 15-12. Courtesy John Ramsay.*

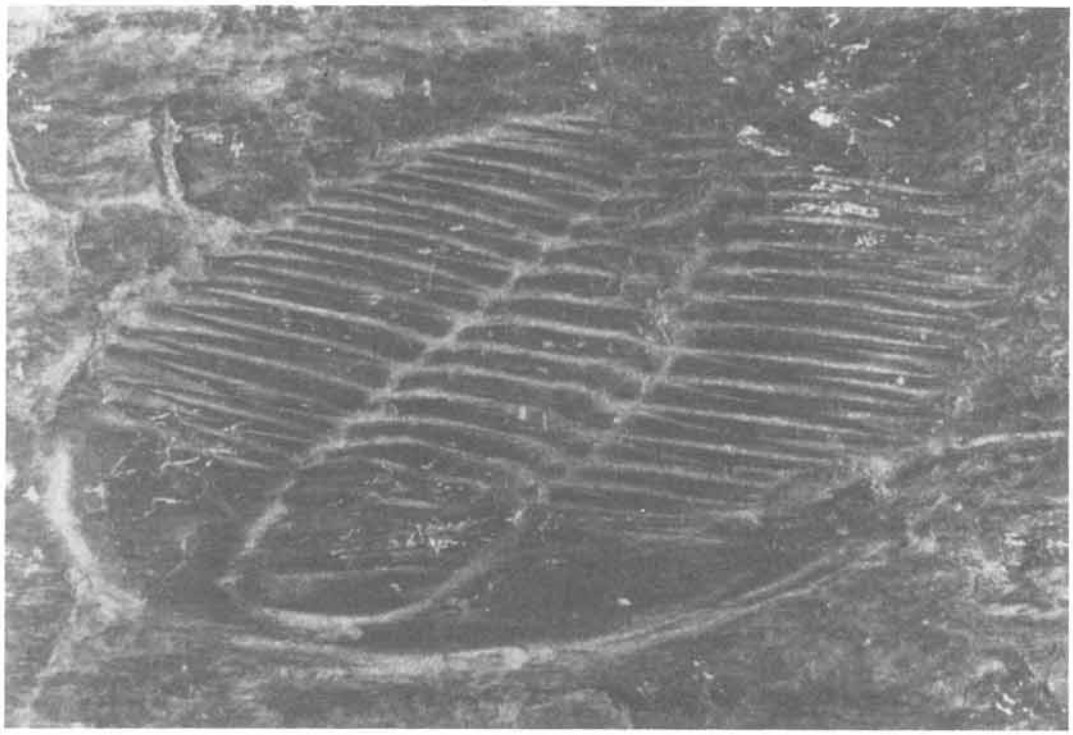

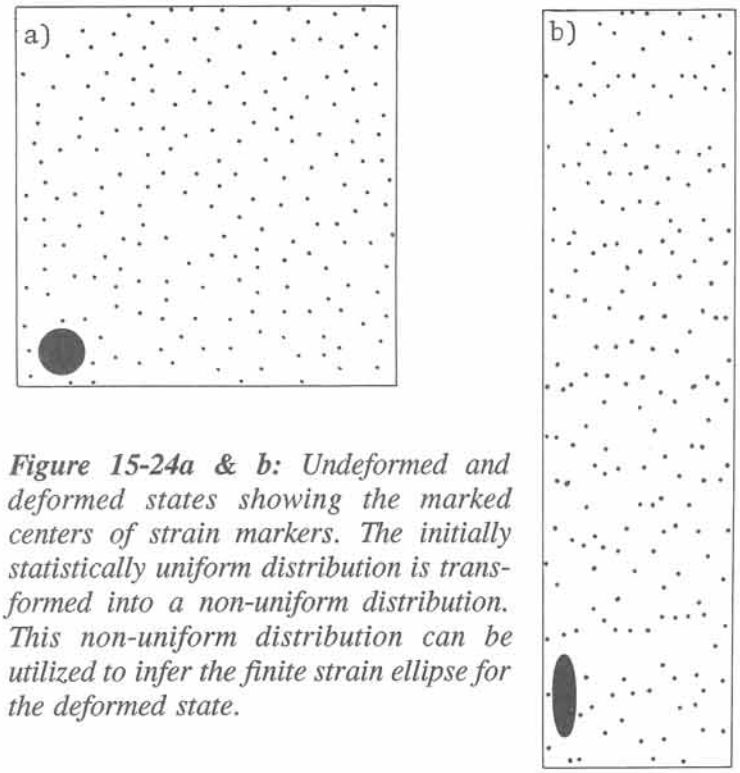

Figure 15-24a & b: Undeformed and deformed states showing the marked centers of strain markers. The initially statistically uniform distribution is transformed into a non-uniform distribution. This non-uniform distribution can be utilized to infer the finite strain ellipse for the deformed state.

15-10 Fry and tieline methods for spaced centers

Rocks may not always contain bilaterally symmetric fossils nor linear or elliptical or spherical markers. An additional method of strain analysis uses the spacing between the centers of pebbles, ooids, or mineral grains. The elementary assumption is that the initial distances between the centers of the objects used were statistically equal in the undeformed state (Fig. 15-24a). After the deformation, the distribution of the center-points is no longer uniform (Fig. 15-24b) and, thus, provides a means to infer the shape and orientation of the strain ellipse for the deformed rocks. The principal techniques used are the Fry method and the tieline method.

The *Fry method* of strain determination is a graphical technique. The center-points of the objects in the deformed rock are first marked. A transparent overlay is marked with a small cross in the center (Fig. 15-25a). The cross will be the center of the Fry plot,

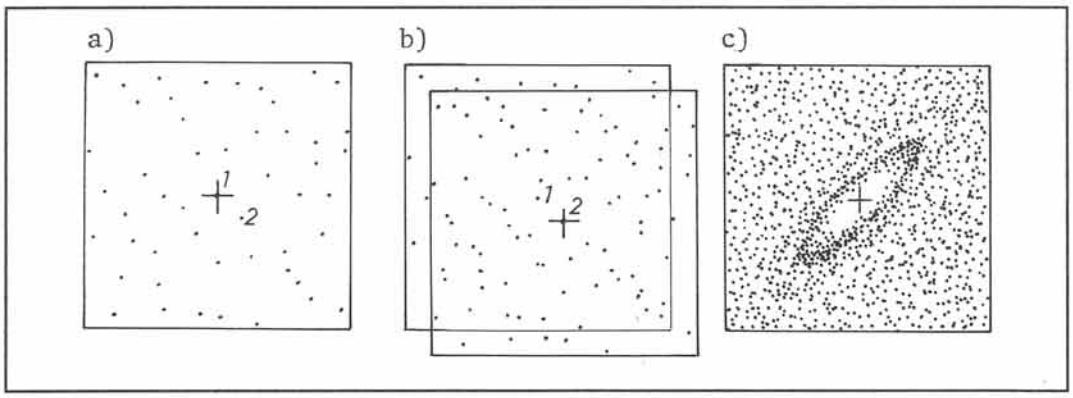

***Figure 15-25:** a) to c) Illustration of Fry method to construct the strain ellipse from non-uniformly distributed centers of strain marker objects. The so-called Fry plot (c) outlines the strain ellipse on a transparent overlay. On this overlay are numerous dots, obtained by shifting the central cross to match with any particular strain marker center. All surrounding centers are then marked on the overlay, before repeating the procedure for each center point in the original set of strain markers (a & b).*

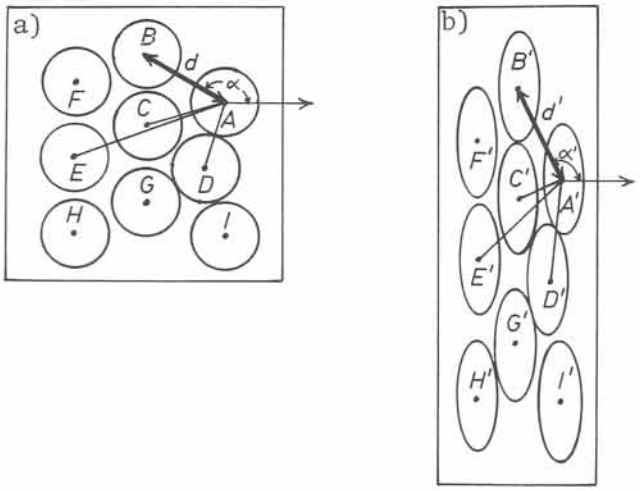

Figures 15-26a & b: *The tieline-method takes an arbitrary reference center in the deformed state and measures the orientation and length of tielines to the centers of all other grains in a half circle space around the reference center. In the undeformed state, the pairs of angles and lengths will be uniform (if the initial fabric is uniform), but this is not so in the deformed state (see Figure 15-26c).*

which collects all marked points on the overlay and leaves a blank area around the plot center, imaging the strain ellipse. The plot is generated by matching the center of the overlay with one of the marked objects and copying all other object-centers onto the overlay. The procedure is repeated many times by shifting the center of the overlay to match with the next object, marking again all other object-centers on the overlay (Fig. 15-25b). A strain ellipse image emerges in the center of the Fry plot (Fig. 15-25c).

The *tieline method* or *center-to-center method* was developed earlier than the Fry method, which is simpler but less accurate. The tieline method chooses one reference center and then plots the distances of all other object-centers within a half circle-space around it (Fig. 15-26a & b). The 180-degrees of the arbitrary half circle-space are subdivided into two halves of +90° and -90°. The measurements are plotted in a graph of the direction angles against the distances to other object-centers in those directions (Fig. 15-26c). A line of best fit reveals a low and a high in the mean distance for particular directions. The high marks the direction and length of the L_1-direction. The low in the curve of mean distances gives the orientation and length of the L_3-direction. The ellipticity is equal to $R_S = L_1/L_3$.

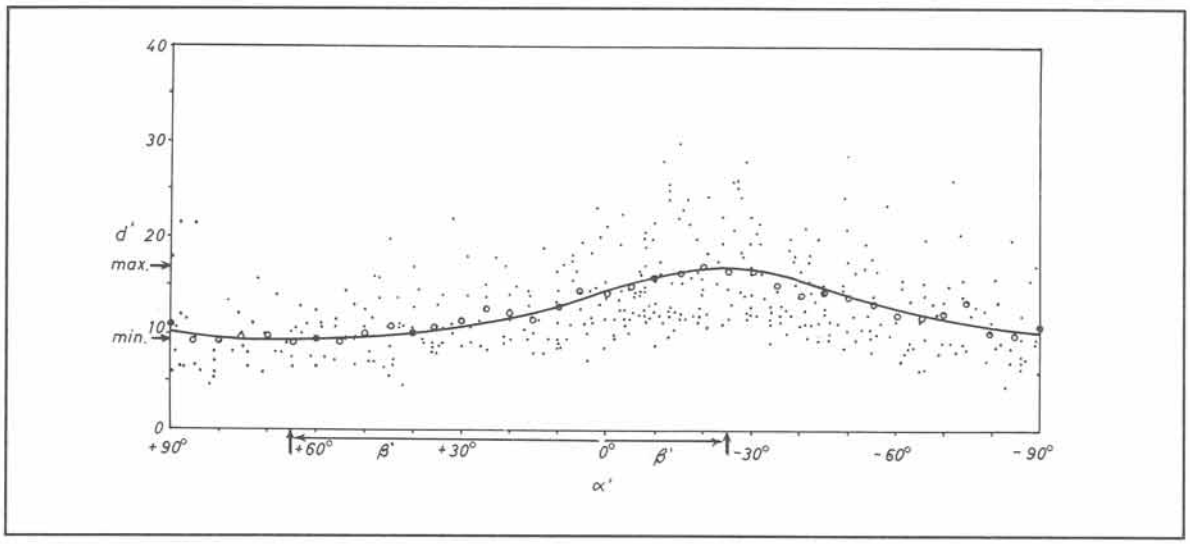

Figure 15-26c: *Plot of tieline measurements graphing the orientations, α, of tielines versus their absolute length, d. See text.*

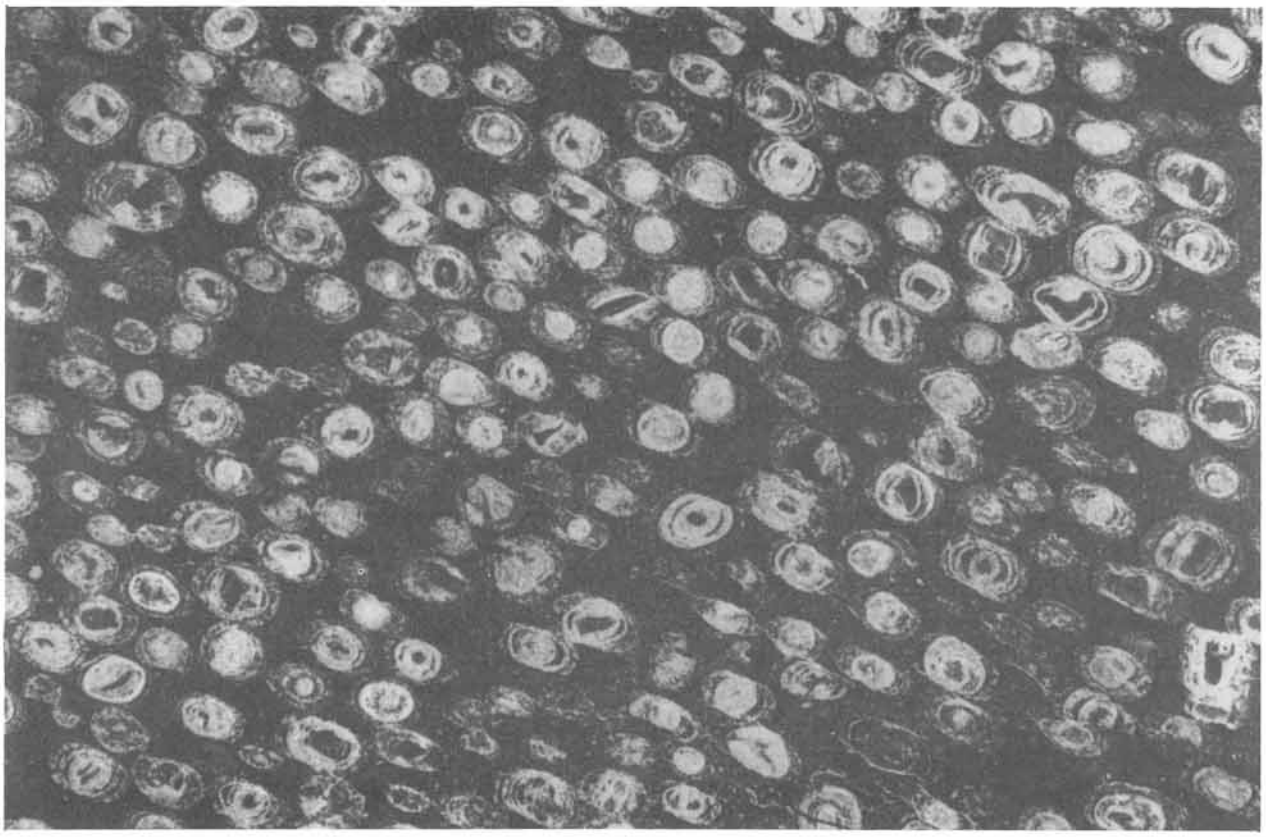

Figure 15-27: *Thin section micrograph of oolitic limestone deformed by pressure solution. See exercise 15-13. Courtesy John Ramsay.*

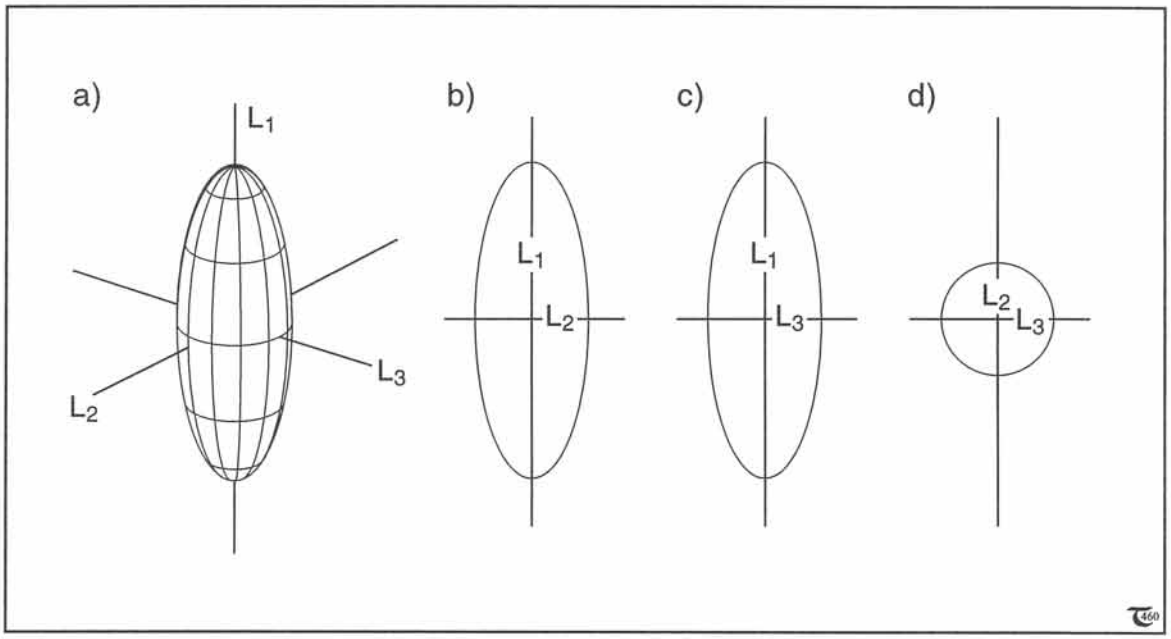

Figure 15-28: *a) to d) Prolate strain ellipsoid and scaled sections of the principal planes.*

☐Exercise 15-13: The oolitic limestone of Figure 15-27 is deformed by pressure solution of matter in distinct seams. The (R_f,ϕ)-method of strain analysis does not work, because the margins of the ooids are partly removed by the solution transfer. a) Use the Fry-method to obtain the shape and orientation of the strain ellipse. b) Determine the strain again, using the tieline-method. c) Do you think the strain-memory of the ooids is complete?

15-11 Oblique sections of prolate strains

One complication, associated with strain determinations of rocks in natural outcrops, is that the surface of exposure does not necessarily coincide with any of the principal planes of strain. It is, therefore, worthwhile to assess how the various types of strain ellipsoids appear in arbitrary cross-sections. Consider a rock volume, comprising deformed ooids that were initially perfect spheres. Exclude any volume change. Three cases of strain are considered below in turn (prolate, oblate, and plane strain).

Figures 15-28a to d illustrate the *prolate* ooid and the three characteristic sections coinciding with the principal planes. The measurement of the two principal stretches in the principal planes of strain is straightforward. The long axis of the ooid is L_1 and the short axis is L_3; for isochoric prolate strains $S_1=(L_1/L_3)^{2/3}$ and $S_3=(L_3/L_1)^{1/3}$ [using $L_2=L_3$ in eqs. (15-7a & c)].

The ellipticity of the principal ellipse of prolate strain is $R_S=S_1/S_3=L_1/L_3$.

The plane of view in natural outcrops may not always follow the principal planes of strain. Any arbitrary section, oblique through the center of the prolate ooid, would contain L_3, because the prolate shape is an ellipsoid of revolution about the L_1-axis. The length of the long axis of the ellipse in the arbitrary section, L_1, depends upon the angle, ϕ, between $L_{1\ REDUCED}$ and the plane of section (Fig. 15-29a):

$$L_{1\ REDUCED}=(L_1^2\cos^2\phi+L_3^2\sin^2\phi)^{1/2} \qquad (15\text{-}14)$$

The ellipticity of the ellipse will be $R_{S\ REDUCED}=L_{1\ REDUCED}/L_3$ and is, in arbitrary sections, always

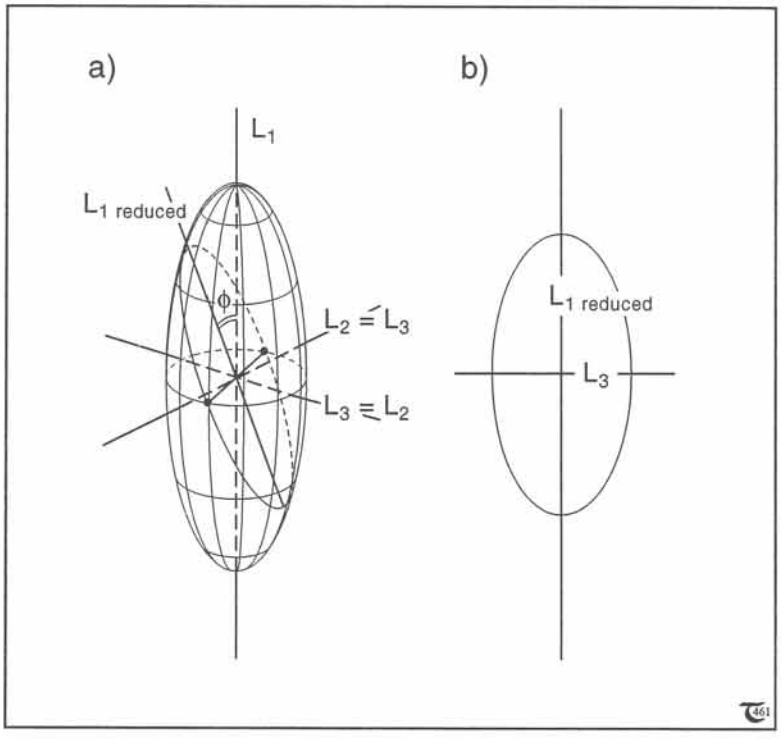

***Figure 15-29:** a) Orientation of oblique section inside prolate strain ellipsoid. b) Plan view of the oblique section. Equation (15-14) quantifies $L_{1\ REDUCED}$, and equation (15-15) allows calculation of the true strain ellipticity, R_s, if angle ϕ (indicated in the strain ellipsoid) is known.*

equal to or smaller than the true ellipticity (Fig. 15-29b). More specifically, for prolate strains, arbitrary sections may show ellipticities, varying between L_1/L_3 and unity. Sections off-center, but at angle ϕ to L_1, will show ellipticities equal to that of a section through the center for the same ϕ. For, although the sectional area of the ooid cut will be smaller, the long and short axis of the ellipses are reduced proportionally, without affecting R. Using the facts, that $L_{1\ \text{REDUCED}} = R_{S\ \text{REDUCED}} \times L_3$ and $R_S = L_1/L_3$ yields:

$$R_S = [(R^2_{S\ \text{REDUCED}} - \sin^2\phi)/\cos^2\phi]^{1/2} \qquad (15\text{-}15)$$

Equation (15-15) allows recovery of the true strain ellipticity, R_S, from strain measurements in oblique sections, provided ϕ is known. It follows that the maximum ellipticity, R_S, occurs always for $\phi = 0°$, when $R_S = R_{S\ \text{REDUCED}}$.

15-12 Oblique sections of oblate strains

Figures 15-30a to d illustrate a perfect *oblate* ooid and the three typical sections coinciding with the principal planes. The measurement of the two principal stretches in the principal planes is straightforward; oblate strains without volume change have $S_1 = (L_1/L_3)^{1/3}$ and $S_3 = (L_3/L_1)^{2/3}$ [using $L_1 = L_2$ in eqs. (15-7a & c)]. The ellipticity of the principal ellipse of oblate strain is $R_S = S_1/S_3 = L_1/L_3$.

Any arbitrary section oblique through the center of the oblate ooid would certainly contain L_1, because the oblate shape is an ellipsoid of revolution about the L_3 axis. The length of the short axis of the ellipse in the arbitrary section, $L_{3\ \text{INCREASED}}$, depends upon the angle, ϕ, between L_1 and the plane of section (Fig. 15-31a):

□Exercise 15-14: Strain analysis on an outcrop of deformed pebbles has yielded an ellipticity $R_S = 2$. Careful study of the outcrop indicates the pebbles define a perfect L-tectonite. The surface in which the ellipticity was measured is at 45° with respect to the maximum extension direction, indicated by the long axis of the pebbles. Calculate the true ellipticity of the principal plane of the strain ellipsoid.

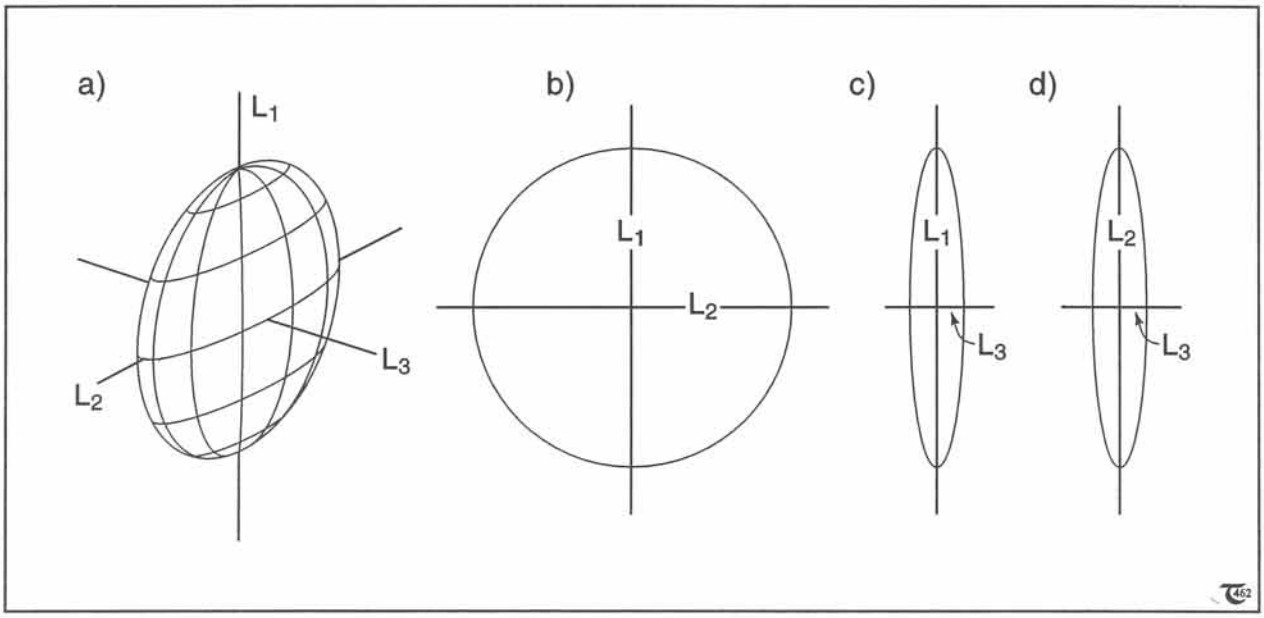

Figure 15-30: a) to d) Oblate strain ellipsoid and scaled sections of the principal planes of strain.

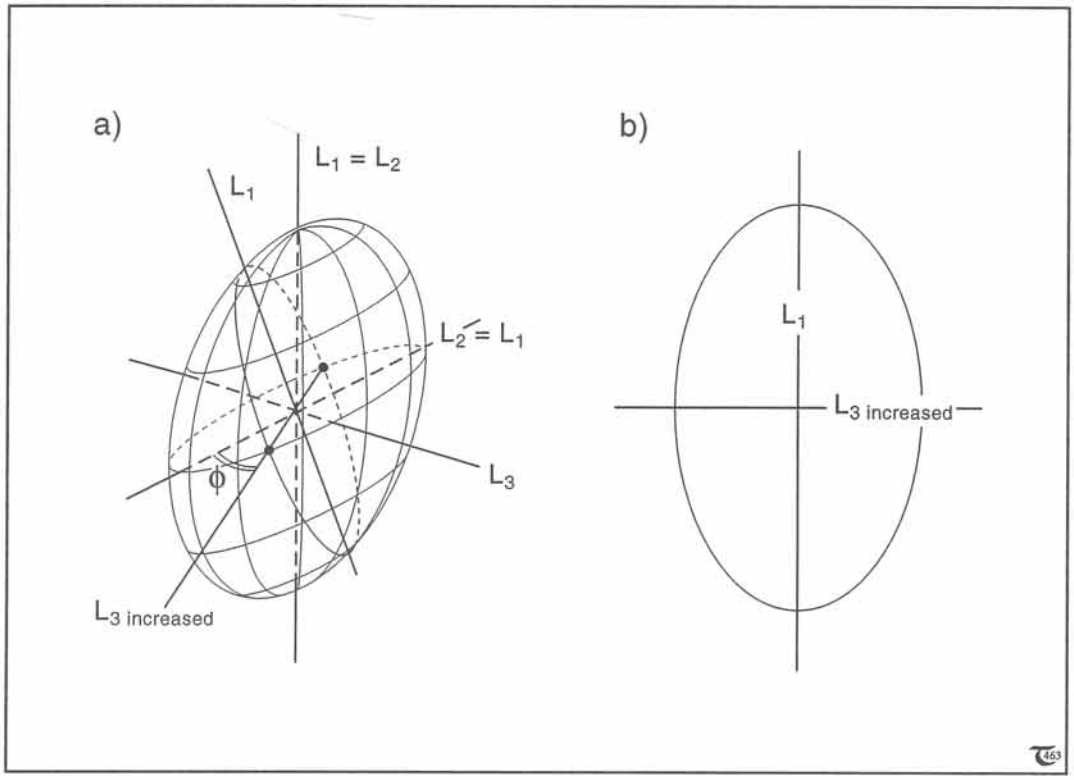

Figure 15-31: *a) Orientation of oblique section inside oblate strain ellipsoid. b) Plan view of the oblique section. Equation (15-16) quantifies* $L_{3\ INCREASED}$. *See exercise 15-15.*

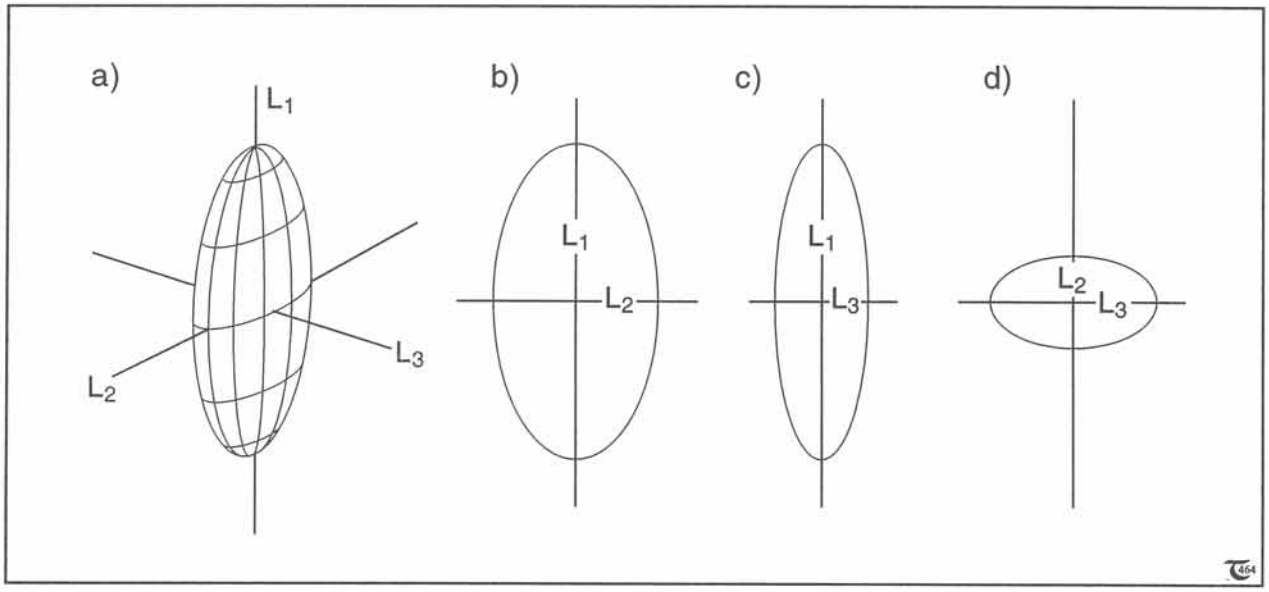

Figure 15-32: *a) to d) Plane strain ellipsoid and scaled sections of the principal planes of strain.*

$$L_{3\,INCREASED} = (L_1^2 \cos^2\phi + L_3^2 \sin^2\phi)^{1/2} \quad (15\text{-}16)$$

The ellipticity of the ellipse will be $R_{S\,REDUCED} = L_1/L_{3\,INCREASED}$ and is, in arbitrary sections, always equal to or smaller than the ellipticity in the L_1-L_3 plane (Fig. 15-31b). More specifically, for oblate strains, arbitrary sections may show ellipticities, varying between L_1/L_3 and unity.

□Exercise 15-15: Derive an expression similar to equation (15-15) but that allows solving R_S for oblique sections through oblate strain ellipsoids.

15-13 Oblique sections of general strains

Figures 15-32a to d illustrate an ooid of *plane strain*, intermediate in shape between the oblate and prolate ellipsoids of revolution. The plane strain ellipsoid itself is not a body of revolution - all three principal axes have different lengths. The stretches in the principal sections follow directly from $S_1 = (L_1/L_3)^{1/2}$ and $S_3 = (L_3/L_1)^{1/2}$ [see eqs. (15-3a & b)]. In fact, everything which follows here is valid not only for a plain strain ellipsoid, but, also, for oblique sections of any general ellipsoid. The ellipticity of the principal ellipse of general strain is $R_S = S_1/S_3 = L_1/L_3$ [using eqs. (15-7a &c)].

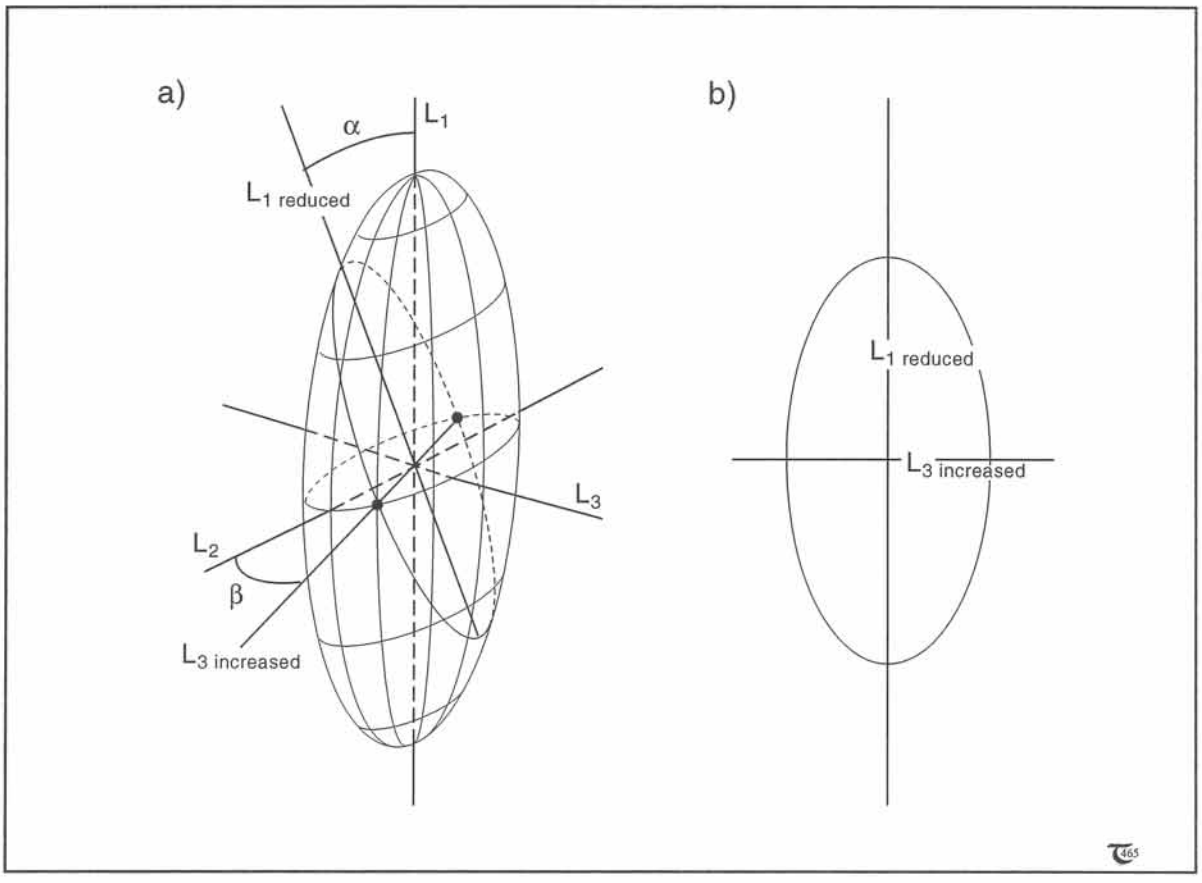

Figure 15-33: *a) Orientation of oblique section inside plane strain ellipsoid. b) Plan view of the oblique section. Equation (15-17a & b) quantifies $L_{1\,REDUCED}$ and $L_{3\,INCREASED}$, respectively. See exercise 15-16.*

Any arbitrary section, oblique through the center of an ooid of plane strain shape, would comprise the following axial lengths (Fig. 15-33a):

$$L_{1\,\text{REDUCED}} = (L_1^2\cos^2\alpha + L_3^2\sin^2\alpha)^{1/2} \quad (15\text{-}17a)$$
$$L_{3\,\text{INCREASED}} = (L_2^2\cos^2\beta + L_3^2\sin^2\beta)^{1/2} \quad (15\text{-}17b)$$

Consequently, the ellipticity of the ellipse will be $R_{S\,\text{REDUCED}} = L_{1\,\text{REDUCED}}/L_{3\,\text{INCREASED}}$ and is, in arbitrary sections, always equal to or smaller than the ellipticity in the L_1-L_3 sections (Fig. 15-33b). More specifically, for plane strain, arbitrary sections may show ellipticities, varying between L_1/L_3 and unity, which occurs for $\beta = 0°$ and α such that $L_{1\,\text{REDUCED}} = L_2$.

In conclusion, arbitrary sections through the center of deformed ooids show elliptical shapes with ellipticities ranging between unity and the maximum values reached in sections containing the major and minor stretching axes. It is useful to compare the strain ellipses, seen on differently oriented surfaces in the same outcrop, to establish which section is closest to that of the L_1-L_3 section. If there is any angle between the stretching lineation and the plane of strain analysis, equations (15-14) to (15-17) may be used to obtain the corrected lengths of the principal directions of the strain ellipse from the reduced ellipticity, measured in oblique sections.

□Exercise 15-16: a) Derive an expression to obtain R_S from oblique sections through the general strain ellipsoid of Figure 15-33a. b) Argue why, contrary to the common assumption in structural geology, plane strain is partly more complex to deal with than either ideal oblate or ideal prolate strains.

15-14 Strain analysis in 3D

The practical analysis of 3D strains is possible making use of the methods for the analysis of 2D strains, outlined in sections 15-7 to 15-10. The strain ellipticities, thus established, may need correction if obtained from marker objects on rock surfaces that are oriented oblique to the principal axes of strain. The angular relationship between such rock surfaces and the principal axes of the bulk strain ellipsoid can be assessed qualitatively using the tectonite concept outlined in sections 15-2 and 15-3. Additional methods to check whether the deformation was by perfect plane strain are outlined in sections 15-4 and 15-5. Once the general shape and orientation of the principal strain axes have been established, the angles α and β between the principal axes and the plane of study must be measured (Fig. 15-33a). Subsequently, the strain estimates made on planar rock slabs oblique to the principal directions of the strain ellipsoid can be corrected, using the expressions given in sections 15-11 to 15-13 (and in the solution of exercise 15-16a).

References

A. Books

Structural Analysis of Metamorphic Tectonites (1963, McGraw-Hill), by F.J. Turner and L.E. Weiss. A very good, early work on the structural analysis of metamorphic rocks with many excellent illustrations.

The Techniques of Modern Structural Geology. Volume 1: Strain Analysis (1983, Academic Press), by J.G. Ramsay and M.I. Huber. Beautifully illustrated and clearly writtten account on strain analysis with many detailed theoretical and practical exercises.

Geological Strain Analysis (1988, Pergamon Press), by R.J. Lisle. A practical booklet with first hand knowledge on the advanced (R_f,ϕ)-technique.

B. Articles

Cloos, E. (1947, *Geological of Society America Bulletin*, volume 58, pages 843 to 918). Oolite deformation in South Mountain Fold, Maryland.

Weijermars, R. (1987a, *Annales Geophysicae*, volume 5B, pages 201 to 210). The construction of shear strain profiles across brittle-ductile shears. Preliminary estimates of conventional shear strain-rates for the Truchas and Palomares Shears (Spain) and the Alpine Fault (New Zealand).

Weijermars, R. (1987b, *Journal of Structural Geology*, volume 9, pages 139 to 157). The Palomares brittle-ductile shear zone of southern Spain.